ELSEVIER

Soil Dynamics and Earthquake Engineering 24 (2004) 199–223

SOIL DYNAMICS AND EARTHQUAKE ENGINEERING

www.elsevier.com/locate/soildyn

Estimating site-specific strong earthquake motions

F. Heuze[a,*], R. Archuleta[b], F. Bonilla[b], S. Day[c], M. Doroudian[d], A. Elgamal[e], S. Gonzales[c], M. Hoehler[a], T. Lai[e], D. Lavallee[b], B. Lawrence[f], P.-C. Liu[b], A. Martin[b], L. Matesic[d], B. Minster[e], R. Mellors[c], D. Oglesby[f], S. Park[f], M. Riemer[g], J. Steidl[b], F. Vernon[e], M. Vucetic[d], J. Wagoner[a], Z. Yang[e]

[a]*Lawrence Livermore National Laboratory, Livermore, CA 94550, USA*
[b]*University of California at Santa Barbara, Santa Barbara, CA, USA*
[c]*San Diego State University, San Diego, CA, USA*
[d]*University of California at Los Angeles, Los Angeles, CA, USA*
[e]*University of California at San Diego, San Diego, CA, USA*
[f]*University of California at Riverside, Riverside, CA, USA*
[g]*University of California at Berkeley, Berkeley, CA, USA*

Accepted 7 November 2003

Abstract

The Campus Earthquake Program (CEP) of the University of California (UC) started in March 1996, and involved a partnership among seven campuses of the UC—Berkeley, Davis, Los Angeles, Riverside, San Diego, Santa Barbara, Santa Cruz—and the Lawrence Livermore National Laboratory (LLNL). The aim of the CEP was to provide University campuses with site-specific assessments of their earthquake strong motion exposure, to complement estimates they obtain from consultants according to the state-of-the-practice (SOP), i.e. Building Codes (UBC 97, IBC 2000), and Probabilistic Seismic Hazard Analysis (PSHA). The Building Codes are highly simplified tools, while the more sophisticated PSHA is still somewhat generic in its approach because it usually draws from many earthquakes not necessarily related to the faults threatening the site under study.

Between 1996 and 2001, the site-specific studies focused on three campuses: Riverside, San Diego, and Santa Barbara. Each campus selected 1–3 sites to demonstrate the methods and procedures used by the CEP: Rivera Library and Parking Lots (PL) 13 and 16 at UCR, Thornton Hospital, the Cancer Center, and PL 601 at UCSD, and Engineering I building at UCSB. The project provided an estimate of strong ground motions at each selected site, for selected earthquake scenarios. These estimates were obtained by using an integrated geological, seismological, geophysical, and geotechnical approach, that brings together the capabilities of campus and laboratory personnel. Most of the site-specific results are also applicable to risk evaluation of other sites on the respective campuses.

The CEP studies have provided a critical assessment of whether existing campus seismic design bases are appropriate. Generally speaking, the current assumptions are not acknowledging the severity of the majority of expected motions. Eventually, both the results from the SOP and from the CEP should be analyzed, to arrive at decisions concerning the design-basis for buildings on UC campuses.
Published by Elsevier Ltd.

Keywords: Earthquakes; Strong motions; Vertical seismic arrays; Seismic syntheses; Empirical Green's functions; Theoretical Green's functions; Nonlinear soil dynamics; probabilistic seismic hazard analyses; Building codes

1. Introduction

The Campus Earthquake Program (CEP) combined the expertise that exists within the University of California (UC) system in geology, seismology, geophysics, and geotechnical engineering, to estimate the earthquake strong motion exposure of UC facilities. These estimates draw upon recent advances in hazard assessment, seismic wave propagation modeling in rocks and soils, and dynamic soil testing.

The procedure starts with the identification of possible earthquake sources in the region and the determination of the most critical fault(s) related to earthquake exposure of the campus. Combined geological, seismological, geophysical, and geotechnical studies are then conducted to

* Corresponding author. Tel.: +1-925-423-0363; fax: +1-925-423-6907.
E-mail address: heuze@llnl.gov (F. Heuze).

0267-7261/$ - see front matter Published by Elsevier Ltd.
doi:10.1016/j.soildyn.2003.11.002

characterize each campus with specific focus on the location of particular existing or planned buildings of special interest to the campus administrators. Deep boreholes are drilled, sampled, and geophysically logged, next to the target structure, to provide in situ measurements of subsurface material properties and to install up-hole and down-hole 3-component seismic sensors capable of recording both weak and strong motions. The boreholes provide access below the soil layers, to deeper materials that have relatively high seismic shear-wave velocities. Analyses of conjugate down-hole and up-hole records provide a basis for optimizing the representation of the low-strain response of the sites. Earthquake rupture scenarios of identified causative faults are combined with the earthquake records and with nonlinear soil models to provide site-specific estimates of surface strong motions at the selected target locations.

For each campus, the strong motion studies consisted of two phases. Phase 1 included initial source and site characterization, drilling, sampling, geophysical logging, installation of the seismic station, and initial seismic monitoring [1–3], and Phase 2 was comprised of extended seismic monitoring, dynamic soil testing, calculation of estimated site-specific earthquake strong motions at depth and at the surface, and, where applicable, calculation of the response of selected buildings to the CEP-estimated strong motions [4–6].

2. Source characterization

Extensive seismo-tectonic reviews were performed first, for the three campuses. These reviews drew from numerous other studies in Southern California [7]. They resulted in the selection of a source and earthquake moment magnitude (M_w) which would create the most serious hazard for each campus, as follows: a M_w 7.0 event on the San Jacinto fault for UCR, a M_w 6.8 event on the North Channel—Pitas Point Fault for UCSB, and a M_w 6.9 event on the Rose Canyon fault for UCSD. The respective shortest distances to the main causative faults

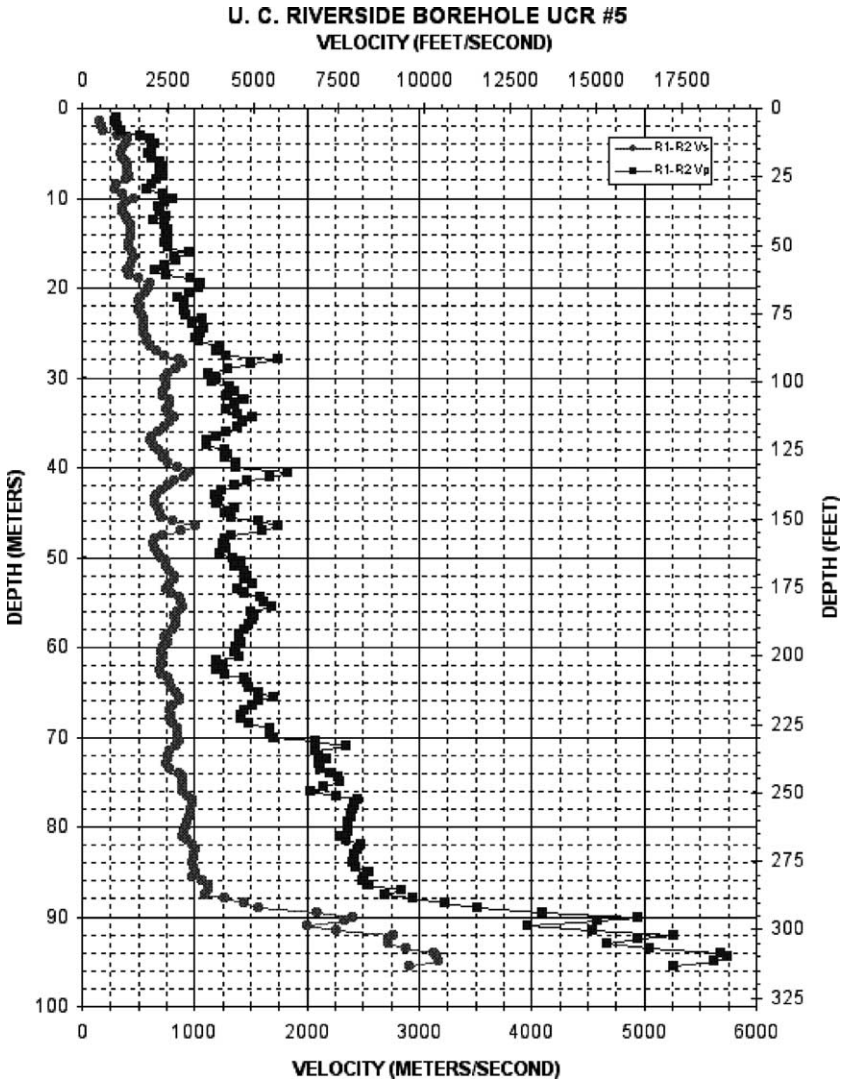

Fig. 1. P and S-wave velocity profiles at the location of the UCR new seismic station.

are 9 km at UCR, 5 km at UCSB, and 3–4 km at UCSD. So, all three campuses are in the near-source region of a potentially damaging rupture.

3. Site characterization

The characterization of the sites first included reviews of previous geologic and borehole data. Typically, these former studies, tailored to building foundation design, involved shallow boreholes, say less than 20-m deep, and minimal soil testing (SPT only). They did not provide the information required to estimate strong earthquake surface motions, i.e. depth to bedrock, lateral and vertical distribution of soil formations, shear and compressional wave velocity profiles, and nonlinear stress-strain behavior of the soils under cyclic loading.

The new CEP studies included seismic refraction surveys, gravity surveys (UCR), cone-penetration tests, and the drilling/sampling/logging of deep holes on each campus. These deep boreholes were the most valuable aspects of the site characterizations because they allowed the following:

- recovery of soil samples from depth exceeding 90 m, for laboratory testing;
- logging of the holes with suspension tools to provide P and S-wave, resistivity, and gamma, profiles;

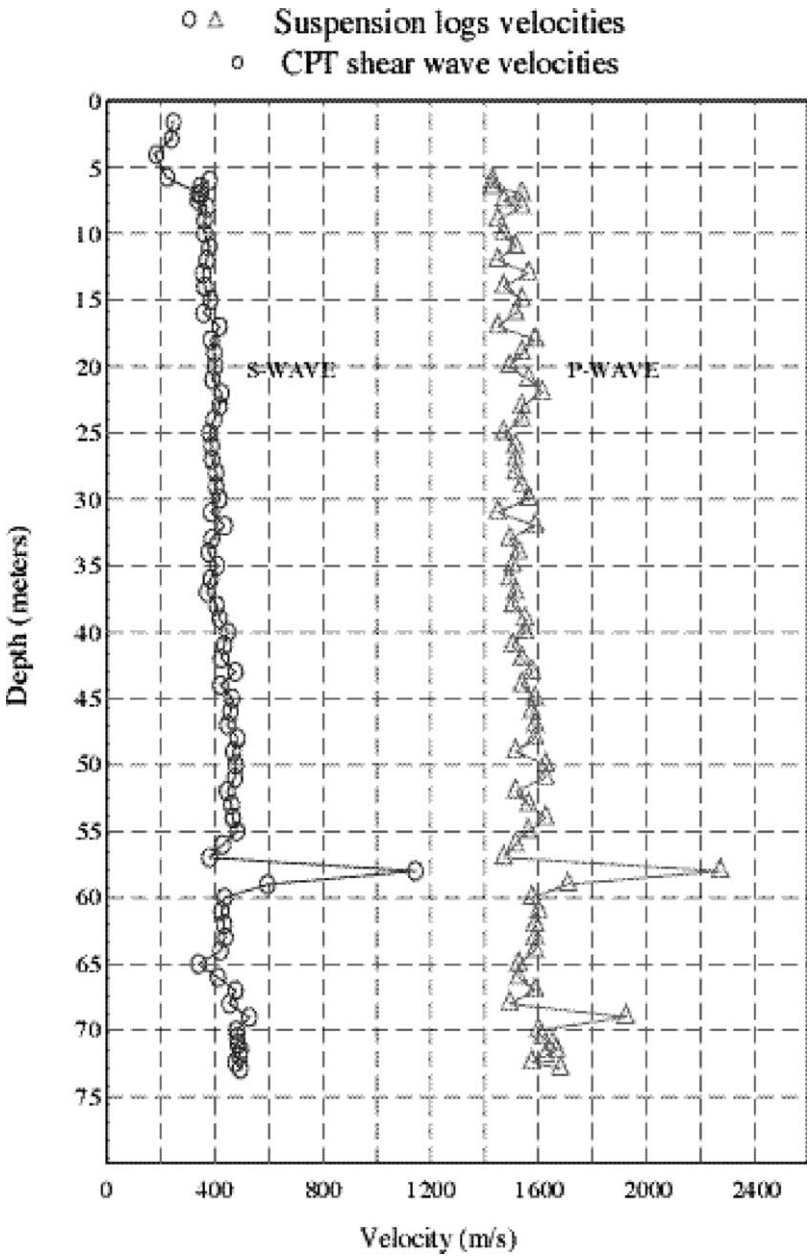

Fig. 2. P and S-wave velocity profiles at the location of the UCSB new seismic station.

- emplacement of 3-component seismometers at depth, thus creating a vertical seismometer array on each campus.

At UCR, three deep holes were drilled encountering the granite basement at depths from 75 to 109 m. The bowl shape of that basement was further outlined from the gravity surveys. The P and S-logs (Fig. 1) revealed the depth of the water table where a P-velocity increase was not matched by an increase in S-velocity (ex: depth of 71 m in Fig. 1). The wave velocity profiles were very comparable to depths in excess of 60 m for sites several hundred meters apart.

At UCSB, the investigations revealed the properties of the Sisquoc claystone formation that uniformly underlies the campus under a few meters of surface cover. Fig. 2 shows the small gradient of velocity increase with depth. This trend is consistent with results from oil well velocity logs to depths of several hundred meters in the Santa Barbara Channel.

At UCSD, the characterization studies defined the layered nature of the site (Fig. 3). Electrical resistivity and gamma logs were very useful complements to the velocity logs. All the geophysical logs showed consistent profiles for the three new borehole sites, separated by up to 1 km (Fig. 4).

4. Laboratory soil testing

While the full description of the soils at the three campuses is given in the specific reports [4–6], Tables 1–3 give a summary description.

Soil samples obtained from the deep holes were tested for cyclic stress strain response using the UCLA Dual-Specimen Simple-Shear system [8], the improvement of which was supported in part by the CEP. Typical results (for the UCSD samples) are shown in Fig. 5 in terms of the reduction of the secant shear modulus, G_s, and variation of the equivalent viscous damping ratio, λ, with cyclic shear strain γ. The main purpose of testing the reduction of G_s with γ was to construct the laboratory normalized modulus reduction curve, $G_s/G_{max}-\log\gamma$, where G_{max} is taken as G_s at $\gamma = 0.0001\%$. The shape of the $G_s/G_{max}-\log\gamma$ curve

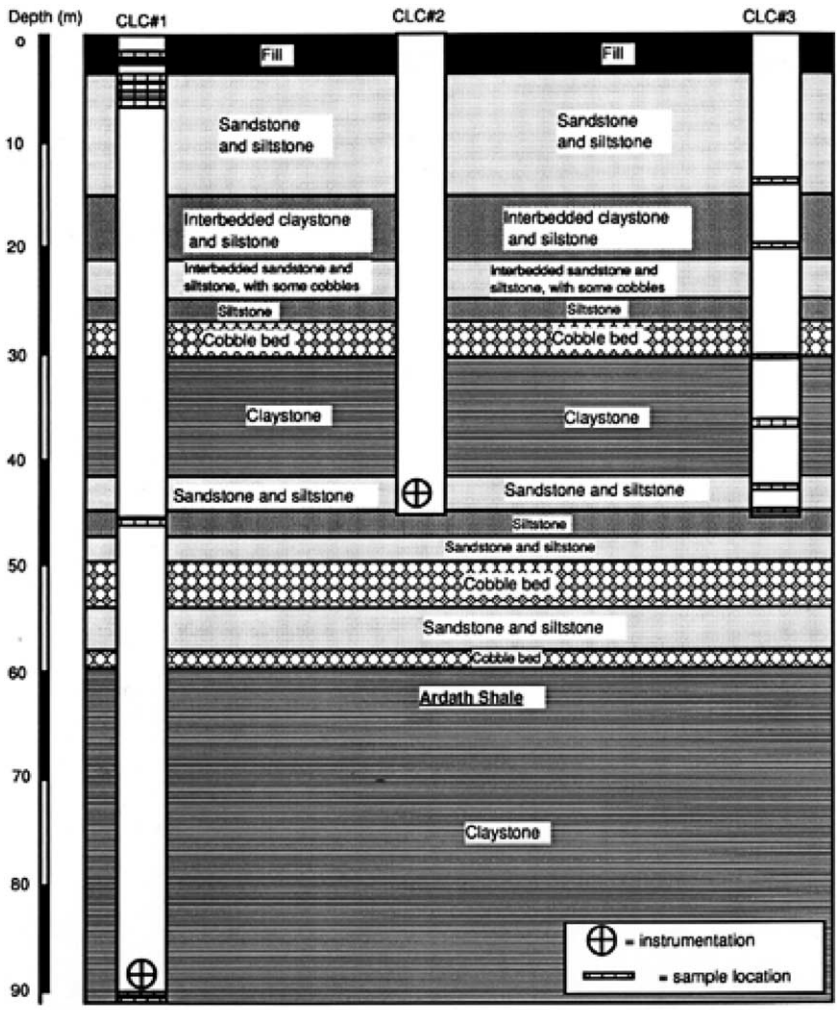

Fig. 3. Soil profile of the site of the new seismic station at UCSD.

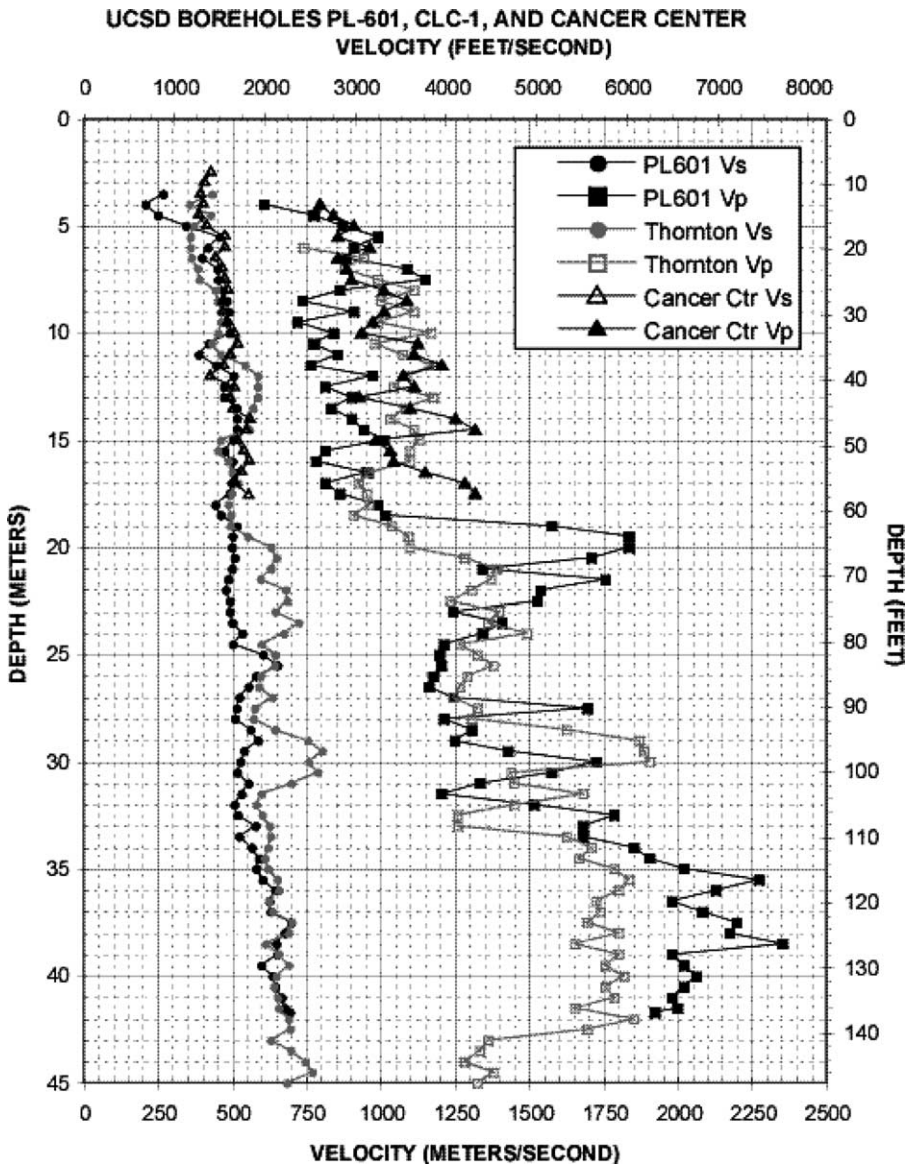

Fig. 4. Comparison of P- and S-velocity suspension logs for three sites on the UCSD campus.

depends mainly on the type of soil and relatively little on the soil disturbance, confining stress and overconsolidation ratio [9,10]. It is also practically independent of the rate of straining [11]. This implies that the laboratory and field $G_s/G_{max}-\log\gamma$ curves are similar, and that the field $G_s-\log\gamma$ curves can be obtained by de-normalizing the laboratory $G_s/G_{max}-\log\gamma$ curves by the field G_{max} values derived from the S-wave profiles discussed above. Such an approach to estimate the field cyclic soil properties by combining the field estimates of G_{max} and cyclic laboratory

Table 1
Basic properties and classification of soils from the UCSB seismic station site

Sample label	Depth (m)	Liquid limit	Plasticity index	Unified soil classification	Dry unit weight (kN/m^3)	Water content (%)	Void ratio	Saturation %
SB-4	1.4	–	0	SM (nonplastic silty sand)	16.6	10.6	0.54	51.2
SB-6	1.9	–	0	SM (nonplastic silty sand)	15.4	17.8	0.65	71.5
SB-12	3.7	–	0	SM (nonplastic silty sand)	13.9	27.3	0.86	84.5
SB-32	9.5	92	38	MH (elastic silt)	9.5	61.9	1.79	93.4
SB-68	20.7	83	33	MH (elastic silt)	10.9	52.0	1.42	99.0
SB-102	31.0	82	31	MH (elastic silt)	11.2	47.3	1.35	94.2
SB-212	64.6	81	30	MH (elastic silt)	11.1	46.1	1.36	91.2

Table 2
Basic properties and classification of soils from the UCR seismic station site

Sample label	Depth (m)	Liquid limit	Plasticity index	Unified soil classification	Dry unit weight (kN/m^3)	Water content (%)	Void ratio	Saturation (%)
P-1	2.1	–	0.0	SM (silty sand)	16.9	9.3	0.60	42.7
P-2	3.7	–	0.0	SW-SM (well-graded sand to silty sand)	17.1	16.4	0.61	75.0
P-3	9.5	–	0.0	SM (silty sand)	17.1	9.2	0.58	43.7
P-4	18.1	–	0.0	SW-SM (well-graded sand to silty sand)	17.5	11.9	0.54	60.3
P-5	24.4	26.6	8.2	SC (clayey sand)	17.8	12.0	0.54	62.6
P-7	32.3	28.4	8.0	SC (clayey sand)	19.1	12.4	0.44	79.7
P-8	37.2	–	0.0	SM (silty sand)	16.5	20.7	0.63	90.5

testing is commonly employed in geotechnical earthquake engineering for nonlinear site response computations [12], and is used here for the calculations of the dynamic response of the soils at the three sites under strong earthquake motions.

Since the deep-hole suspension logs and the laboratory tests enable independent estimates of G_{max} shear modulus values, it is informative to compare the two results. This comparison is shown in Table 4. It can be seen that, in spite of the careful sampling (with Pitcher samplers), handling, and testing of the soils, the two estimates can differ by a large factor. There are three main possible reasons for obtaining higher G_{max} in the field than in the laboratory, all of them well recognized in the soil dynamics community. They are sample disturbance, different rates of straining and different confining stresses. In the CEP program the sample disturbance was kept at a minimum and it is reasonable to assume that the effect of the disturbance was small. The rates of loading in the field suspension logging testing were substantially higher than those applied in the laboratory. The cyclic shear strain amplitudes generated during the wave propagation in suspension logging tests are very small (their exact values are not known), and the frequencies are of the order of 1 kHz. In spite of the small cyclic strain amplitudes, such frequencies result in high strain rates, much higher than the strain rates applied in the laboratory and than those generated during earthquakes. However, considering that G_{max} increases 2–10% if the rate of straining is increased 10-fold [11], the effect of the rate of straining alone can account for only a fraction of the difference between the field and laboratory G_{max} values in Table 4. This leaves the difference between the confining stresses in the field during suspension logging and the confining stresses in the laboratory as the main contributor to the discrepancy between G_{max} measured in the field and in the laboratory. It has been shown that confining stress affects significantly the value of G_{max} [13]. While applying the in situ vertical stress in the Dual-Specimen Simple-Shear system it is practically impossible to fully activate the in situ lateral stresses without restructuring (fully disturbing) the soil, especially in the case of pre-consolidated soils which may have relatively large lateral stresses. Consequently, the mean confining stresses in the laboratory were substantially lower than those in the field. In any case, as indicated above, these differences would not significantly change the shape of the assumed field $G_s/G_{max}-\log\gamma$ curves that were used in the site response analyses.

Strength envelopes in consolidated-drained triaxial tests were obtained by UCB for soils from all campuses, to complement the UCLA data that do not cover the stress-strain behavior at large strains at failure. Results for the UCSD samples are shown in Fig. 6 (after Ref. [14]).

5. The new seismic stations and new earthquake records

The new seismic stations became fully operational, respectively, in July 1997 at UCSB, July 1998 at UCSD, and September 1998 at UCR. All stations are capable of

Table 3
Basic properties and classification of soils from the UCSD seismic station site

Sample label	Depth (m)	Liquid limit	Plasticity index	Unified soil classification	Dry unit weight (kN/m^3)	Water content (%)	Void ratio	Saturation (%)
SD-6	1.8	26.9	5.4	CL (ML sandy silty clay)	14.0	8.9	0.90	27
SD-20	6.1	51.8	35.2	CH (fat clay)	16.4	21.8	0.62	95
SD-22	6.7	51.0	33.7	CH (fat clay)	16.3	23.0	0.62	99
SD-47	14.2	57.4	33.3	CH (fat clay)	16.9	20.9	0.60	97
SD-67	20.4	46.2	25.8	CL (lean clay)	16.4	18.1	0.65	77
SD-122	37.2	48.8	25.8	CL (lean clay)	17.4	18.6	0.55	93
SD-299	91.1	49.1	24.2	CL (lean clay)	18.6	15.2	0.45	93

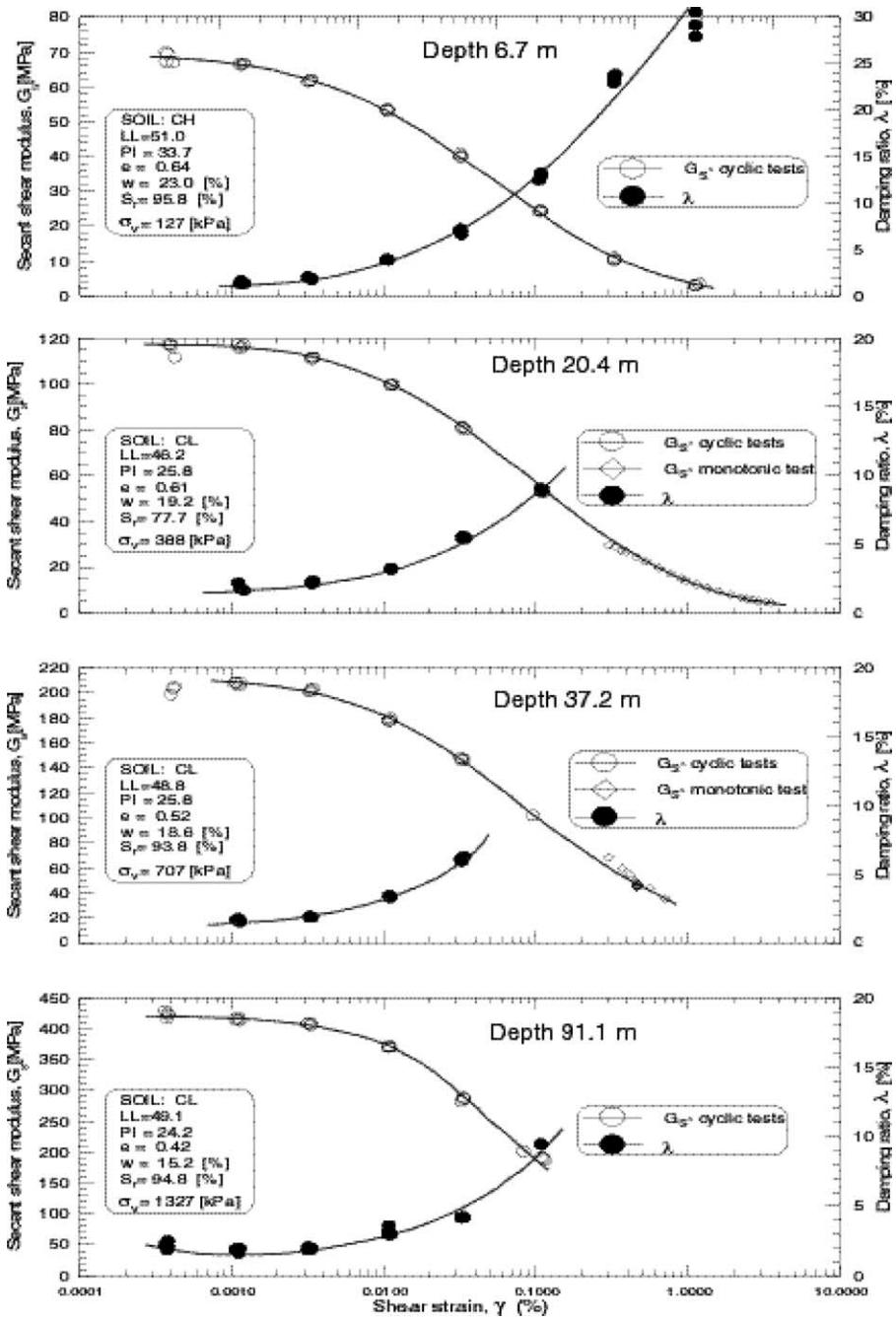

Fig. 5. Typical results of dual-specimen simple-shear tests on samples from UCSD.

recording both weak and strong motions at depth and at the surface. The specific depths and instrument types are summarized in Table 5. As the program developed, the arrangements of the stations evolved. The latest station installed (UCR) was the first for the installation of the new Kinemetrics line of Episensors/Hyposensors. (Trade names are used for completeness and do not imply endorsement of specific products.)

All stations have provided high-quality earthquake records since their inception. These records are also transmitted to the Southern California Earthquake Center where they are accessible by outside researchers. A sample event record from UCSD is shown in Fig. 7. That particular record indicates little modification of the motions between depths of 46 and 91 m. This is generally consistent with the experience from other vertical arrays in the US, in China, and in Japan, where much of the motion modifications seem to develop in the upper 30 m or so of the soil profiles.

6. Site-specific strong motion estimates

The methodology for estimating the surface strong motions is based on a combination of seismological and

Table 4
Ratio of laboratory G_{max} to field G_{max} for three UC campus soils

Campus	Depth (m)	Laboratory G_{max} (GPa)	Field G_{max} (GPa)	Ratio laboratory/field
UCR	2.1	30	55	0.54
	3.7	48	265	0.18
	9.5	46	355	0.13
	18.1	93	405	0.23
	24.4	150	545	0.28
	32.3	220	754	0.29
	37.2	116	619	0.19
UCSB	3.6	38	71	0.54
	9.5	63	221	0.29
	20.7	103	259	0.40
	31.0	133	247	0.54
	64.6	178	239	0.74
UCSD	1.8	12	171	0.07
	6.1	78	259	0.30
	6.7	69	274	0.25
	14.3	138	631	0.22
	20.4	118	803	0.15
	37.2	212	893	0.24
	91.1	430	1649	0.26

geotechnical analytical tools [15]. The seismological calculations are all linear, whereas the geotechnical calculations are nonlinear. The sequence of steps is as follows:

- select a causative fault and a moment magnitude for its rupture;
- model the fault as a rupture surface discretized in many subfault elements;
- populate the fault elements with small events. These are preferably derived from small earthquakes recorded at the site (empirical Green's functions (EGFs)) or, if no event was recorded, the fault elements are populated with theoretical Green's functions. UCR and UCSB fall in the first category and UCSD falls in the second;
- sum up the contributions from these fault elements to simulate motions at the ground surface for a hypothesized rupture scenario (seismic syntheses);
- simulate many different rupture scenarios which each give the same total moment magnitude;
- deconvolve linearly these surface syntheses down to the base of the drilled soil column in materials (rocks, stiff soils) which are assumed to behave linearly even in strong earthquakes;
- propagate the calculated down-hole incident motions up to the surface with nonlinear soil dynamics models.

6.1. Green's function and stochastic source approach

The basic principle used in the linear part of the simulations is the representation theorem [16]. This theorem states that the ground displacement observed at a location is the spatial integral over the fault surface of the temporal convolution of the fault slip time-function with a Green's function. The slip time-function may vary from point to point on the fault, as does the Green's function. This is the basic method used in kinematic modeling of seismic sources. The stochastic source method used in the CEP studies is described in detail in Archuleta et al. [17]. When the Green's function is estimated empirically from recordings of small earthquakes located on the fault surface of interest, the method is referred to as the EGF method. This was the method used for UCR and UCSB. In the absence of EGFs (recorded events) from the Rose Canyon fault, the UCSD study used an analytical Green's Function approach. The Green's Function method has been used extensively for deterministically synthesizing strong ground motion, as well as in inversions for parameters of the source rupture process [18–20].

6.1.1. Validation of the approach

The basic issue of validation is the degree to which a method produces realistic estimates of the ground motion. The measure of ground motion one uses can vary significantly. For example, one could compare computed peak values of ground motion, such as peak acceleration or peak velocity, with those obtained from a specific earthquake. Other comparisons might be between the complete time-histories in phase and amplitude or perhaps between response spectra at different periods. Each measure can be evaluated on an earthquake-by-earthquake basis.

One critical measure for the method is whether the simulated source spectrum approximates the Fourier amplitude source spectrum of large earthquakes [21,22]. We have assumed (based on numerous studies) that a large earthquake has a Fourier amplitude displacement source spectrum which has a characteristic shape, often referred to as ω^{-2} spectrum. In Fig. 8 we compare the source spectrum from our simulation with Brune's ω^{-2} spectrum. Using a different number of subfaults we find that the modeling results are almost independent of the number of subfaults when that number is greater than 3000. For the entire frequency range the source spectrum of the simulated earthquake agrees with Brune's ω^{-2} spectrum. Many EGF models produce a spectral hole near the corner frequency that leads to a serious underestimation of the radiated energy; see discussion in Ref. [19].

As a further assessment, we illustrate how an ensemble of synthetic ground motions based on the method described above can be compared with recorded data-response spectra from the 1994 Northridge earthquake. We take the fault plane and hypocenter as known [23]. For our EGFs we use two aftershocks (Event ID 3147272, 29 Janaury 1994 12:47:36.2, M 3.3; Event ID 3150210, 6 February 1994 13:19:27.0, M 4.1) that were recorded at the same sites as the main shock [24]. In order to compare differences arising from the EGFs, we compute synthetics for the seven stations (three components) that were in common for both

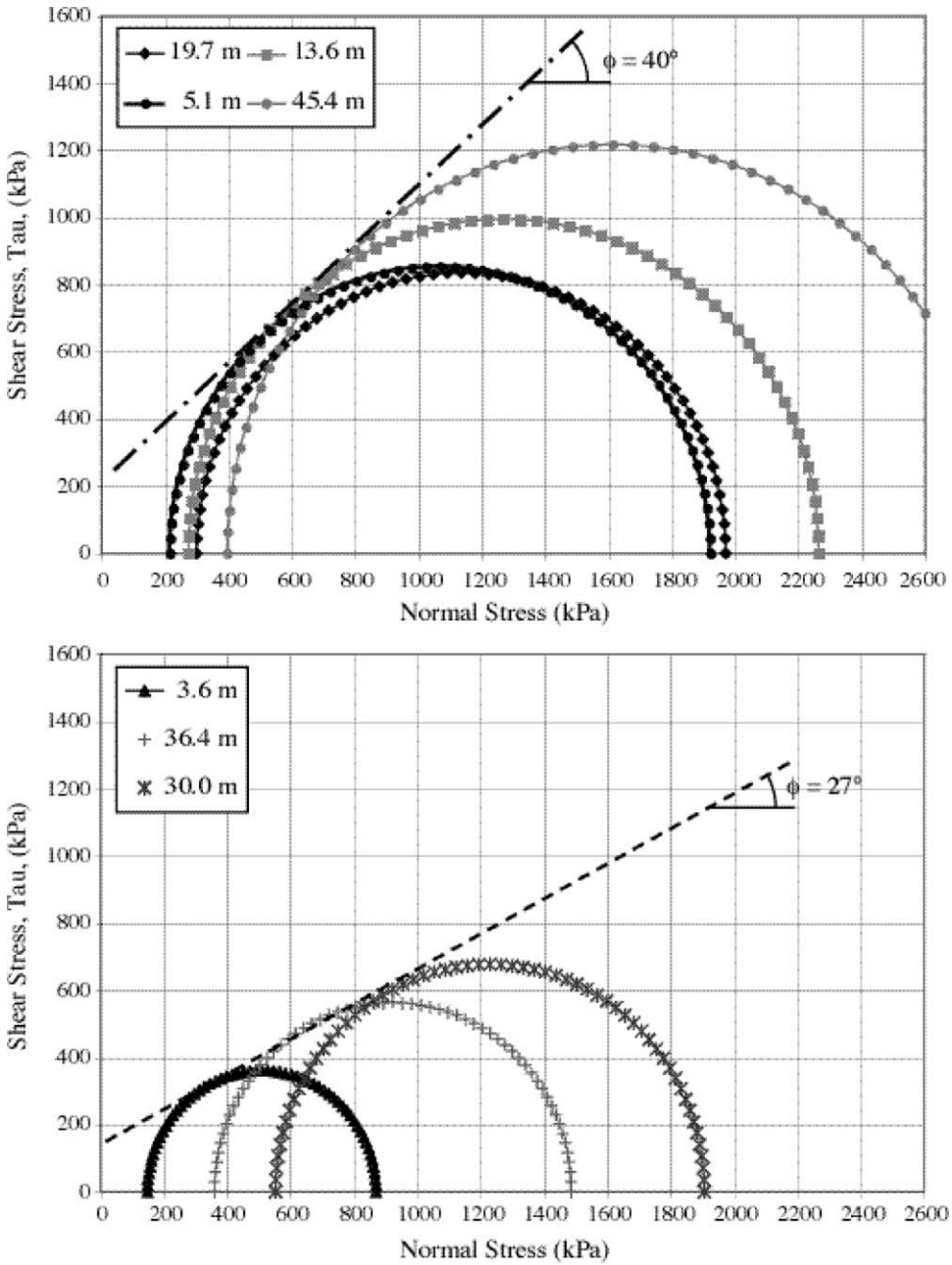

Fig. 6. Strength envelopes from consolidated-drained triaxial tests on UCSD soils.

aftershocks and the main shock with the exception of the record at the Jensen Filtration Plant, main building. This site experienced slumping and its Fourier amplitude spectrum of the main shock shows an order of magnitude loss in spectral amplitude for frequencies greater than 1.0 Hz.

For each EGF we compute 150 synthetic (linear) time-histories of acceleration from which we calculate the mean response spectrum and its standard deviation. As an example of the response spectra, we plot results for two stations, Canoga Park (CPC) and Santa Susana (SSA), in Figs. 9 and 10, respectively. The closest distance to the fault is 15.7 km for Canoga Park, and 18.1 km for Santa Susana. Canoga Park is an alluvial site and Santa Susana is a sandstone rock site. All three components of motion are shown. The solid line is the spectrum of the Northridge record, and the dashed lines represent the ± 1 SD (sigma) of our estimates. Because these stations are located up dip and west of the fault rupture, they will experience some directivity as the rupture moves from the hypocenter toward the surface and from the eastern edge of fault to the western side [23]. These figures are chosen to illustrate the type of variation ($\pm 1\sigma$) in the EGF prediction versus one

Table 5
Seismic station characteristics at the three UC campuses

Campus	Depth (m)	Sensors	Some specs (passband, dynamic range, clip level)	Recorders
UCR	0	3-component Kinemetrics Episensor	0–200 Hz micro-g to 2 g ± 2 g clip level	2 Quanterras 4128, 24-bit, 121 channels
	31.9	3-component Kinemetrics Hyposensor	Same	
	99.1	3-component Kinemetrics Hyposensor	Same	
UCSB	0	3-component Kinemetrics FBA	0–100 Hz 10^{-5} to 2 g ±2 g clip level	Kinemetrics K-2
	0	3-component Wilcoxon accelerometer	0.1–300 Hz micro-g to 0.5 g ± 0.5 g clip level	24-bit Quanterra
	74	3-component Kinemetrics FBA-23	0–100 Hz 10^{-5} to 1 g ± 1 g clip level	Kinemetrics K-2
	74	3-component Wilcoxon accelerometer	0.1–300 Hz micro-g to 0.5 g ± 0.5 g clip level	24-bit Quanterra
UCSD	0	3-component Kinemetrics FBA-23	0–100 Hz 10^{-5} to 1 g ± 1 g clip level	2 RefTek 24-bit RT72A-08 6 channel dataloggers
	0	3-component Wilcoxon accelerometer	0.1–300 Hz micro-g to 0.5 g ± 0.5 g clip level	
	46	3-component Wilcoxon accelerometer	Same	
	91	3-component Wilcoxon accelerometer	Same	

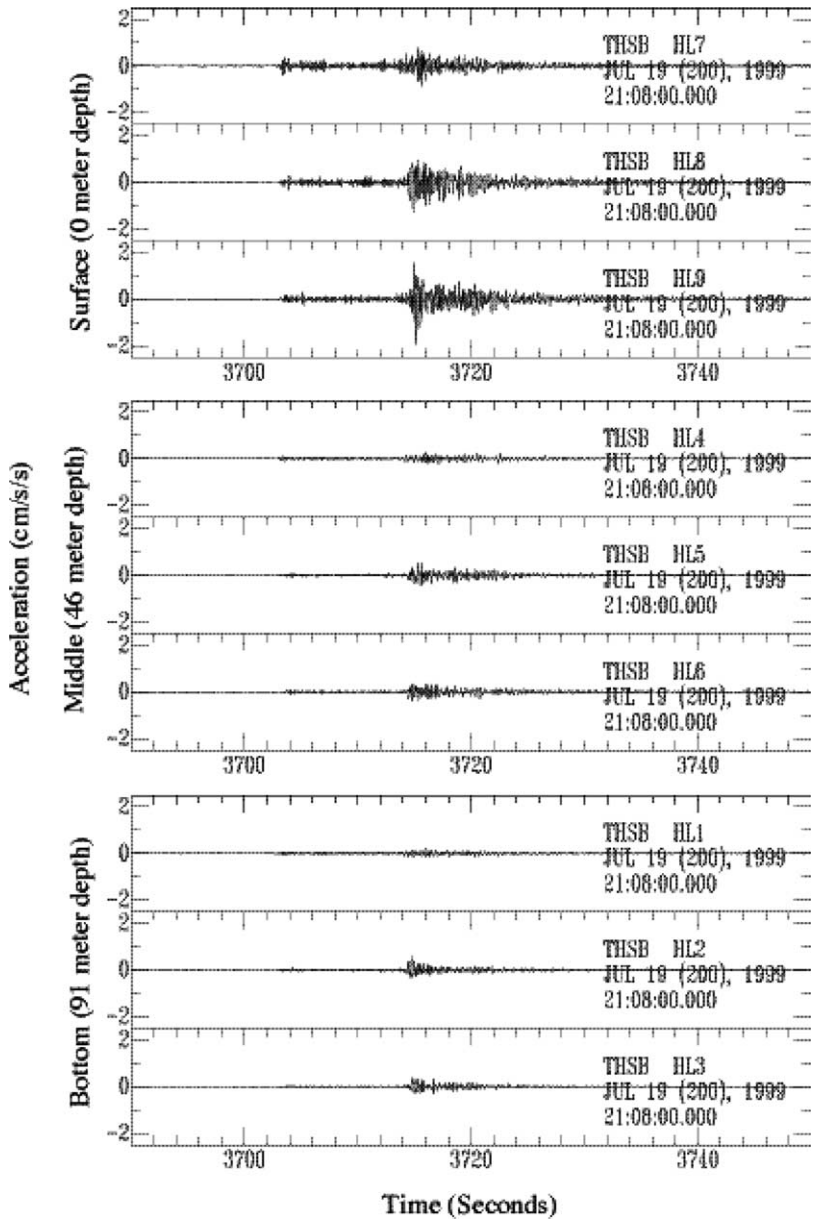

Fig. 7. Record of a M 4.4 event at a distance of 96 km, at the new UCSD seismic station. The vertical channels are 1, 4, and 7.

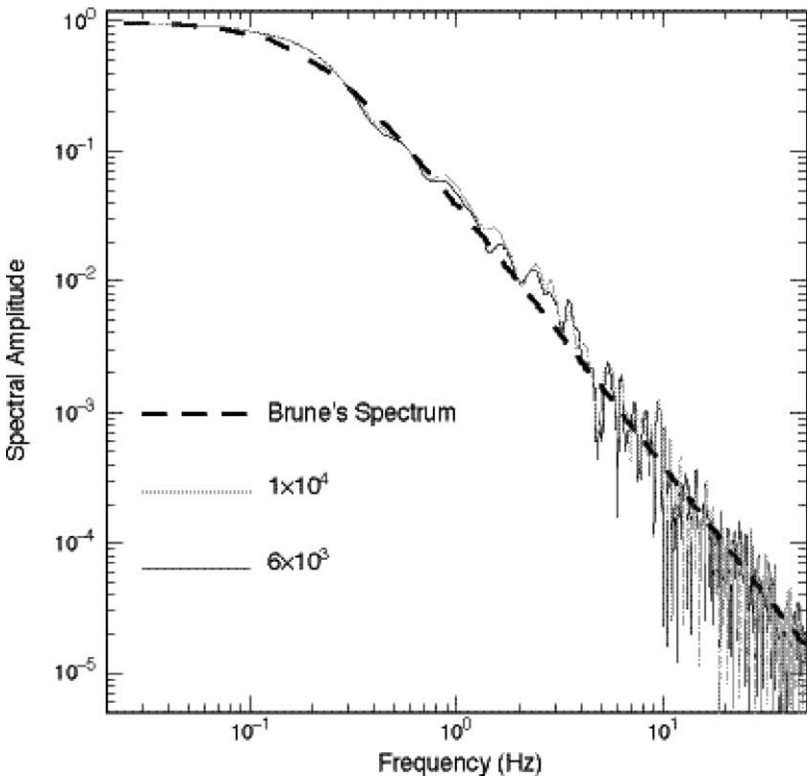

Fig. 8. Comparison of Brune's spectrum with stochastic simulations. The corner frequency is 0.5 Hz. We separately used 3000, 6000, and 10,000 subevents to simulate the Brune's spectrum. For clarity we show results only for the 6000 and 10,000 cases. There is little difference between 3000 and 6000 subevents.

realization of an earthquake for two different soil conditions. By using two different aftershocks as sub-events, the figures illustrate the variation one can expect from the initial spectral content chosen as an EGF. The true variability is summarized by looking at the bias and standard deviation as a function of frequency for all seven stations.

To estimate the modeling error we compute the bias and standard deviation for 5% damped response spectrum [25]. The source model parameters are the seismic moment of the main shock, the corner frequency of the main shock, the average rupture velocity, the fault geometry, and the hypocenter. The average response spectrum is obtained from 150 stochastic source models. For Northridge we fixed the source parameters of the main shock and used two different EGFs. For each EGF we compute the bias and standard deviation for the average of seven stations in the frequency range 0.5–10 Hz (Fig. 11). The standard error for both EGFs is generally less than 0.5; mean values are 0.35 and 0.42 for EGF A and B, respectively. This standard error is consistent with 0.5 found by Hartzell et al. ([25], Fig. 9B) who used similar stations. This error is less than the average standard deviation, about 0.8, determined from six different methods for the 1988 Saguenay earthquake [26]. The bias generally lies between ± 0.5. Our results are the average of 150 simulations where we did not assume any a priori slip distribution as Hartzell et al. [25] did in their comparison with the data. Nonetheless, the bias in the response spectra (Fig. 11) is not that different from that found by Hartzell et al. ([25], Fig. 9b), including the under-prediction of the response spectra at high frequencies. That under-prediction, seen in the negative bias for both EGFs at frequencies greater than 4.0 Hz, may be due to soil nonlinearity that is not accounted for in linear simulations [25].

Another measure of validation is the basic shape and level of ground motion, as compared to that predicted by probabilistic seismic hazard analysis. The probabilistic method represents an average of ground motions from a suite of different earthquakes for the same distance and magnitude as that simulated by the stochastic method. As shown later in our predictions for the UCSB site, the shape and level of the synthetic response spectra agree with the probabilistic ground motions over a broad frequency range when we account for nonlinear wave propagation in the soil.

There are differences between simulations using the two different aftershocks as EGFs, as will also be evident in the synthetics generated for UCSB. These differences reflect modeling uncertainty due to the selection of the EGF. Dan et al. [27] used 17 EGFs to simulate a M 6.7 event (JMA magnitude); they found a standard deviation about 45%. They also found that combining all 17 EGFs into a single computation reduced the coefficient of variation to about

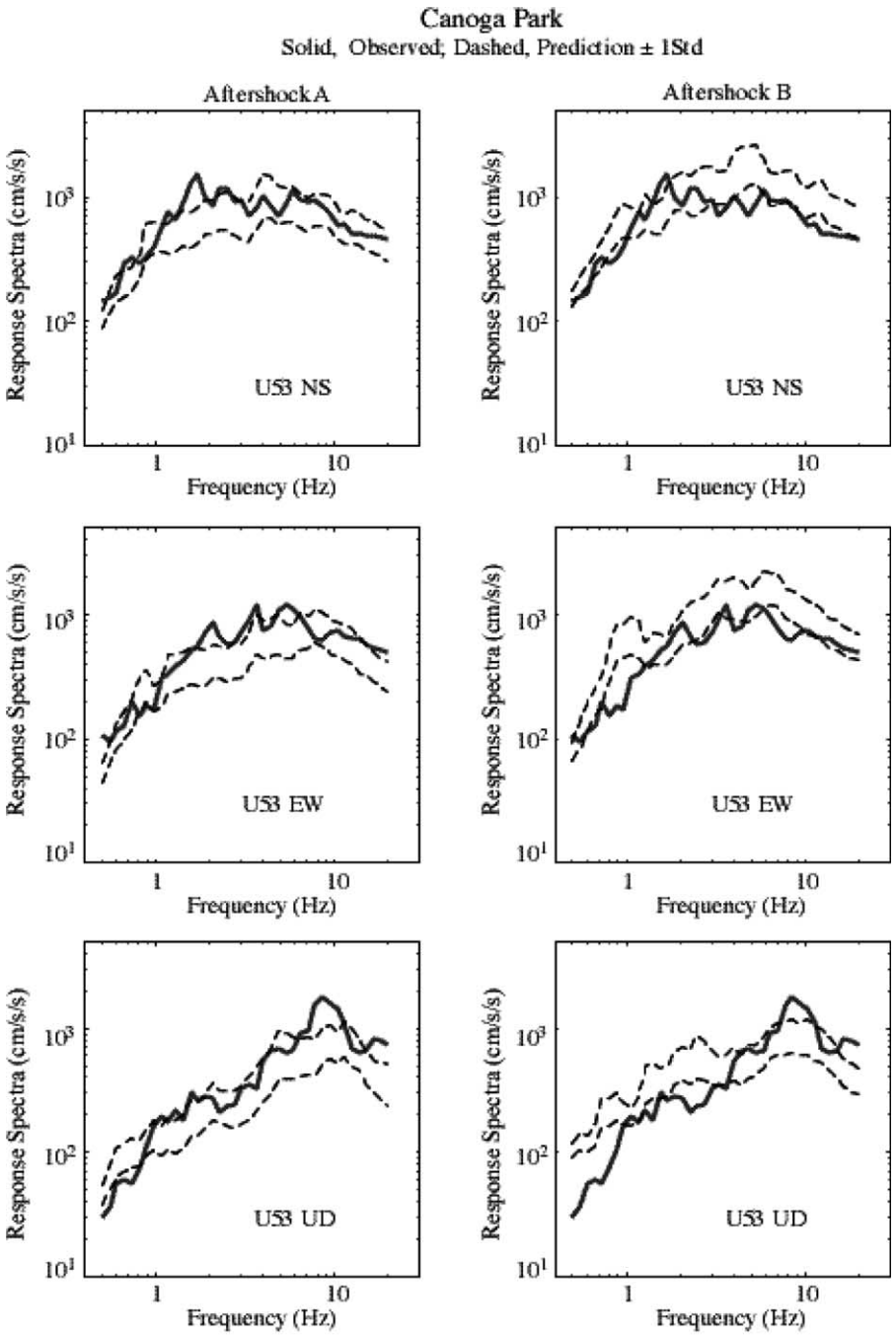

Fig. 9. Comparison of observed and calculated acceleration response spectra for Northridge records at CPC station. Solid line is the observed spectrum. Dashed lines are the synthetic spectra at the mean$\pm 1\sigma$ levels.

15% but systematically under-predicted the peak acceleration, peak velocity and spectral intensity by 12, 11 and 19%, respectively. Jarpe and Kasameyer [28] used EGFs to simulate ground motion at different stations for the Loma Prieta earthquake. Each of the stations had a different number of EGFs available to be used in the synthesis. They found no correlation between the standard error and the number of EGFs used to simulate the ground motion.

As noted by Archuleta et al. [17], the source model we use for ground motion simulations has stochastic components. Among these are random timing variations that are added to the slip initiation time of the model subfaults. One of the model assumptions is that the spatial correlation of these timing variations is negligible. This assumption is probably not an important limitation at short periods (less than ~ 0.5 s) nor at larger distances (exceeding

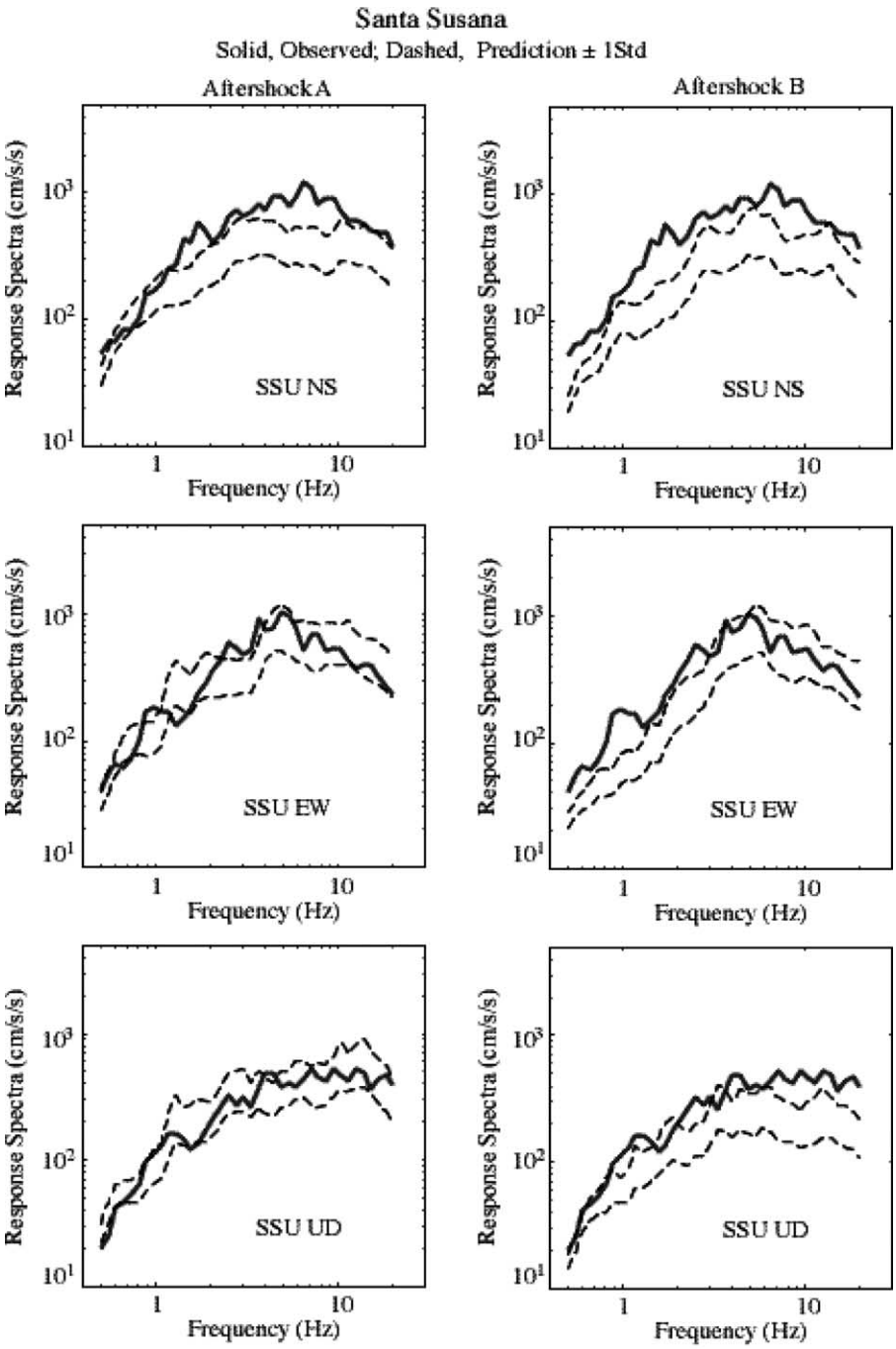

Fig. 10. Comparison of observed and calculated spectra for Northridge records at SSA station. Solid line is the observed spectrum. Dashed lines are the synthetic spectra at the mean ± 1σ levels.

~10–20 km) from the fault; see the validation study in Ref. [17]. At periods exceeding about 0.5 s, however, pulse coherence can lead to enhanced (reduced) near-fault ground motion due to forward (backward) rupture directivity. The directivity effect can be especially important at near-fault sites like Thornton hospital (~5 km from the fault). Empirically, however, the directivity effect is found to be small (less than about 20%) for periods less than 1 s, although it can become quite large at longer periods [29]. Oglesby and Day [30] show that a fault that is highly heterogeneous in its stress distribution, i.e. a fault where there is almost no correlation between regions of high and low stress, greatly diminishes the effects of directivity on the ground motion. They attribute this effect as being mostly due to differences in the average rupture velocity between heterogeneous and smooth faults. The highly heterogeneous

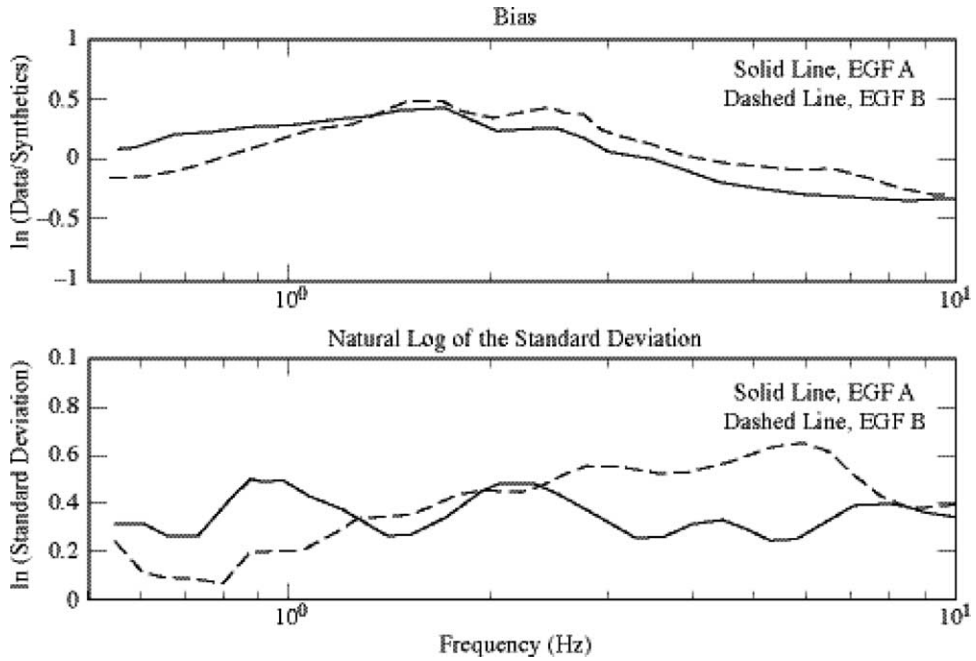

Fig. 11. The bias and standard deviation of the response spectra averaged over seven stations and 150 simulations based on EGFs A and B are plotted against frequency.

faults have a wide range in rupture velocity for a given stress drop, leading to a lower average velocity. In order to account for realistic wave propagation at high frequencies while simultaneously approximating a point source in space and time, the EGF method uses small events. The difficulty with small events is that they have almost no measurable long-period content. Although the effects normally associated with being close to the fault, such as directivity, are present in the kinematic model used to simulate the rupture process, the slip function is convolved with an EGF that has minimal amplitude at periods longer than 2 s. Even if the near-source effects were present in the kinematics of the rupture as they are in our simulations, the convolution using an EGF will effectively minimize them in the final ground motion. Thus the stochastic behavior of the rupture velocity, discussed above, and convolution using an EGF with minimal amplitude at long periods, means that the ground motions for periods longer than 2 s are lower bounds for what might be expected during an earthquake. This is the case for both UCSB and UCR. However, theoretical Green's functions were used to calculate the ground motion for UCSD. In these calculations there is no limitation on the response at any period. It is only the stochastic spatial nature of the rupture velocity and slip that limits the coherence.

6.2. Down-hole strong motions

For each campus, at least 100 fault rupture scenarios were simulated. The results were presented as acceleration response spectra for the mean and the plus and minus one standard deviations of the natural logarithm of the ensemble of motions, for the North–South, East–West and vertical directions. Examples of the results for UCSD, in the EW and NS directions, are shown in Fig. 12. Representative time-histories were also given. It is noteworthy that, typically, the N–S and E–W motions have distinct characters. This reflects the radiation pattern and directivity effects of fault rupture.

6.3. Nonlinear soil dynamics models and validation

The calculations of strong surface motions were made under the assumption of one-dimensional vertical wave propagation of S-H motions from the depth of the down-hole seismic syntheses. Three dynamic nonlinear models available in the U.C. system were selected for these calculations: NOAH (Nonlinear Analysis Hysteretic) by UCSB [24], SUMDES (Sites Under Multi-Directional Earthquake Shaking) by UCD [31], and CYCLIC by UCSD [32].

Nonlinear models cannot be strictly validated against analytical solutions, but they can be compared to each other. To that effect, 3-component down-hole incident time-histories for UCSB were used as input and propagated up the UCSB soil profile with the three codes. In NOAH, which is a finite difference formulation, the intrinsic attenuation (seismic Q) was taken from the UCLA tests at very low strains; it ranged from close to 0 to 2.5%, depending upon the layer. In SUMDES and CYCLIC, both finite element codes, the numerical damping was, respectively, 0.5 and

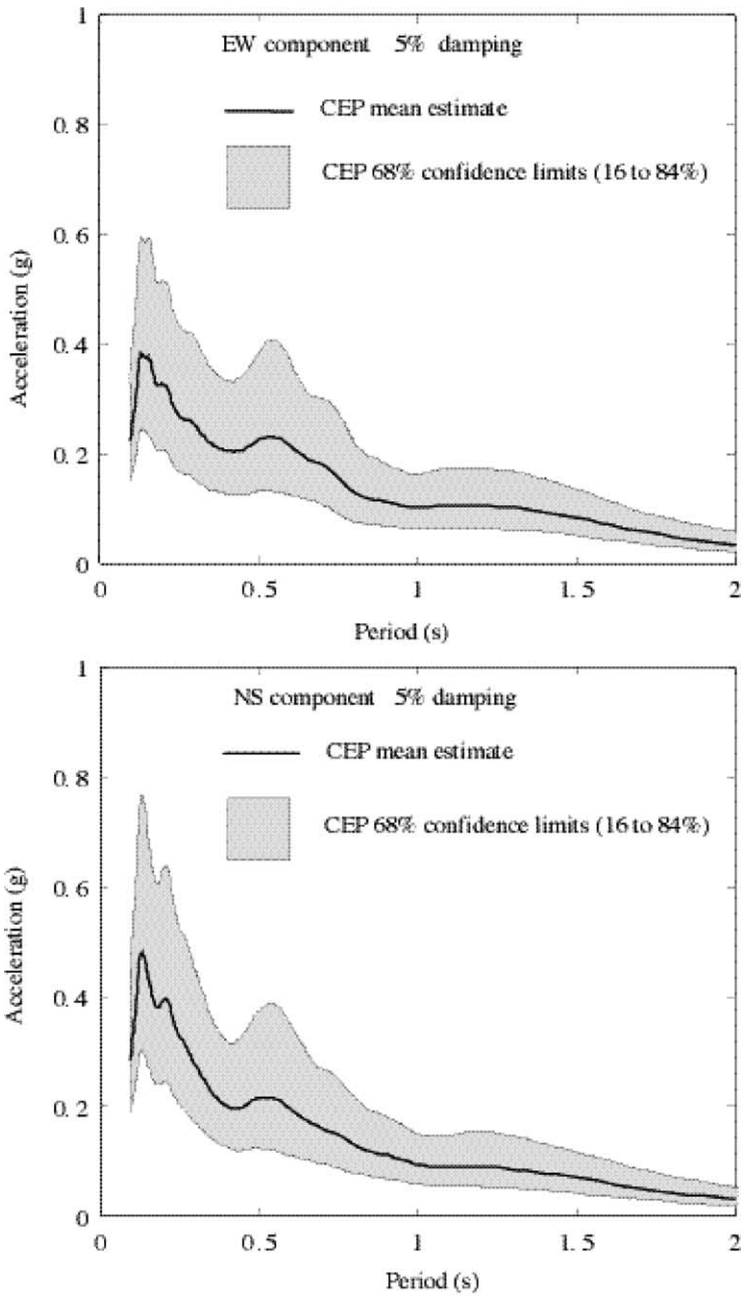

Fig. 12. Acceleration spectra of computed bedrock incident motion (depth 91 m) at UCSD: (a) E–W component; (b) N–S component.

0.8%. In all codes the nonlinear hysteretic damping varied with strain, as determined from the UCLA tests.

A representative example of the comparison of results from the three nonlinear models, for the three components of motion, is shown in Fig. 13, both for the time-histories and for the spectral accelerations. These results are very consistent, thus lending confidence in the models.

6.4. Validation of the soil profiles

The field and laboratory characterization of the campus soils provides a basis for the numerical models of the sites. An example of computational soil profile is given in Table 6. It is that of the UCSD seismic station site (Thornton). The coefficient of earth pressure at rest was $K_0 = 0.5$ for all layers. Moreover, the availability of actual earthquake records at the surface and at depth below these sites provide an opportunity for further checking of the models. This is achieved, for example, by using pairs of up-and-down recordings and determining how well the site model reproduces the down-hole records, given the surface motion time-histories. The down-hole computed signal was obtained by a deconvolution of the signal recorded at the surface. This procedure is illustrated in Figs. 14–16 for

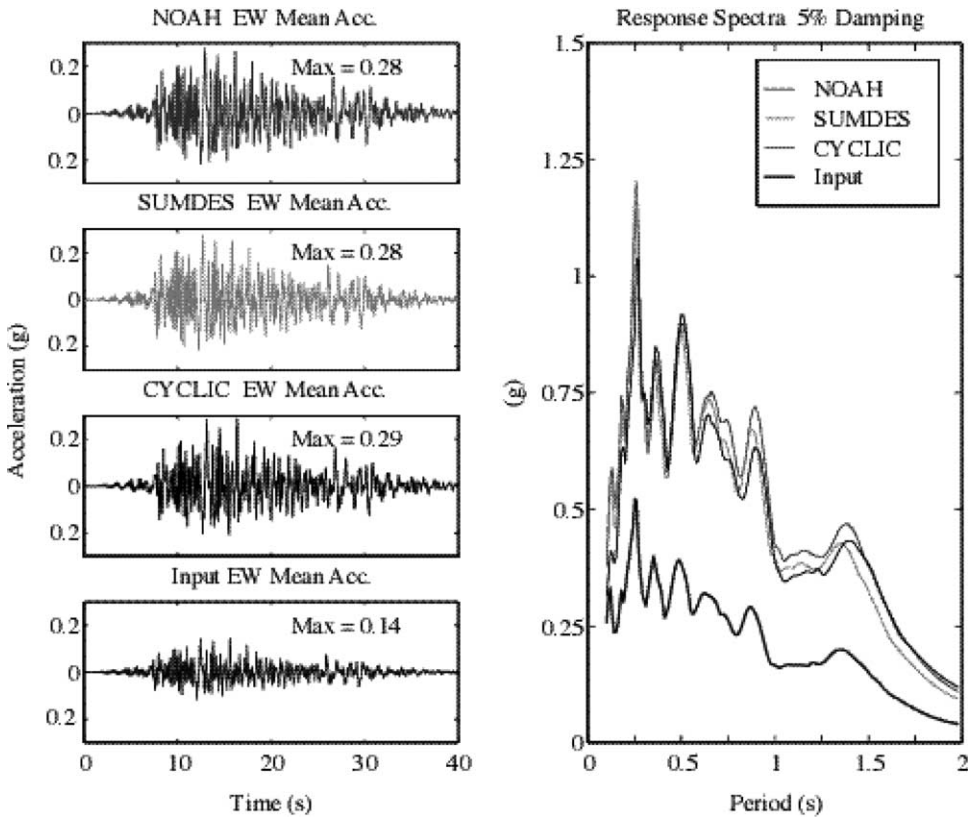

Fig. 13. Comparison of NOAH, SUMDES, and CYCLIC results, for a time-history representative of a mean scenario, EW component, at UCSB.

the three campuses. These show that a one-dimensional vertical wave propagation assumption is quite satisfactory for the three sites. Although, at UCR the difference between calculated and recorded down-hole motions may reflect the effect of the sloping bedrock surface under the site.

6.4.1. Nonlinear behavior of the soils

The CEP estimates of surface motions use nonlinear soil dynamics models because of the presumed nonlinear response of soils to the strong motions. This assumption is corroborated by the level of shear strains expected in the M 6.8 to 7.0 events for the campuses. A representative example (UCR) of profile of maximum shear strain induced in the soil column, versus depth, for a mean and a mean $+1\sigma$ scenario is shown in Fig. 17. In this particular case, it can be seen that maximum cyclic shear strains of about 0.15% are calculated. Based on the laboratory tests results such as shown in Fig. 5 and presented in specific reports [4–6] for this level of cyclic strains, the postulated earthquakes may reduce the secant shear modulus, G_s, of the soils in the top 30 m by up to 80% in a mean scenario and 85% in a $+1\sigma$ scenario.

6.4.2. Estimated surface strong motions

The down-hole motions were propagated to the surface through the nonlinear soil profiles using the NOAH codes for UCR and UCSB, and the CYCLIC

Table 6
Computational soil profile at the Thornton hospital/Cancer Center site

Depth (m)	V_s (m/s)	V_p (m/s)	Unit weight (kN/m^3)	Damping (%)
4	416	870	18.4	2.0
8	410	870	18.4	2.0
11	480	1010	18.4	2.0
14.5	600	1086	18.4	2.0
16.5	520	1160	20.5	2.0
20	520	1030	20.5	2.0
28	630	1290	19.4	2.0
31	805	1750	19.4	2.0
33	610	1450	19.4	2.0
42.5	655	1740	19.4	2.0
48.5	685	1350	20.6	2.0
50	840	1740	20.6	2.0
51.5	750	2050	20.6	2.0
54.5	1050	2700	20.6	2.0
59	695	1928	20.6	2.0
61	1020	2380	20.6	2.0
64.5	716	1911	20.6	2.0
65.5	900	2040	20.6	2.0
68.5	720	1815	20.6	2.0
70.5	820	2100	20.6	2.0
73	820	2020	20.6	2.0
78	735	1870	20.6	2.0
81	840	2000	20.6	2.0
83	895	1930	20.6	2.0
84	966	2202	20.6	2.0
91	850	2020	20.6	2.0

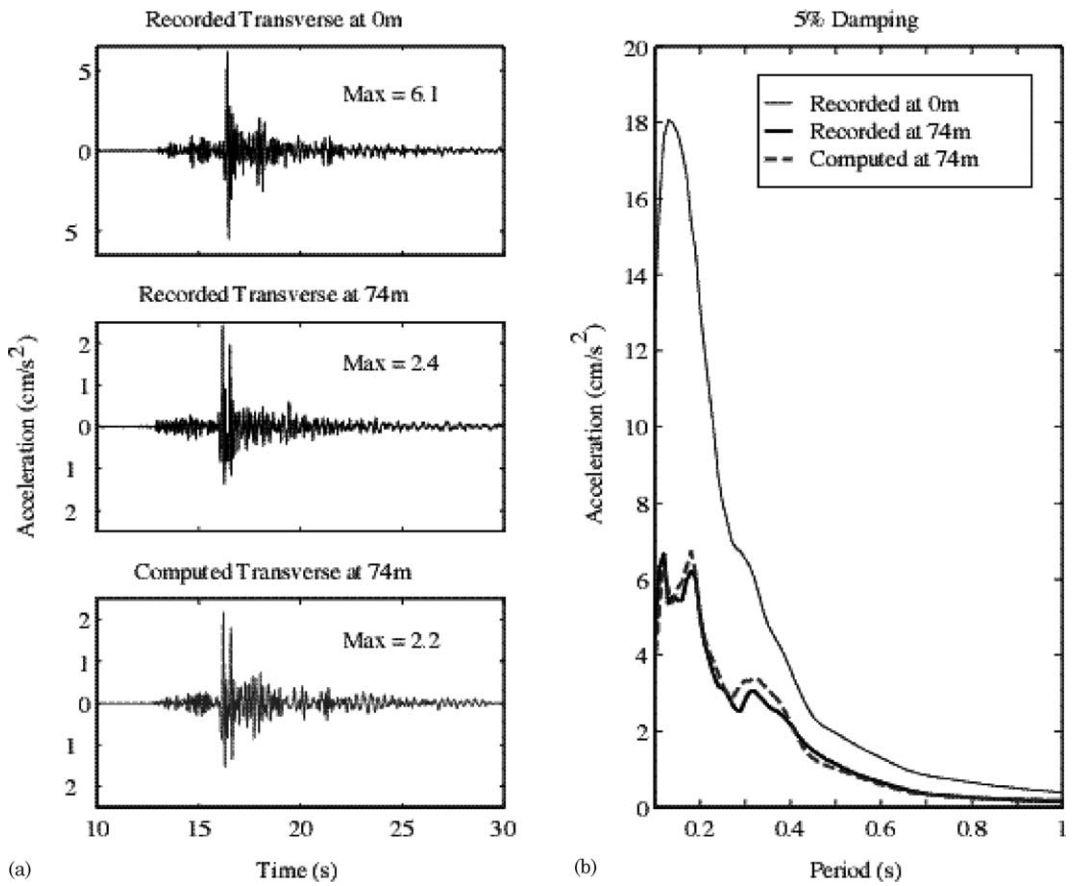

Fig. 14. (a) Comparison of the computed and recorded accelerograms at UCSB, at 74-m depth, for the transverse component. Event of August 15, 1999 (M 3.2 at 11 km). Both the surface and down-hole records were rotated to the transverse direction of the event, to maximize the SH component; (b) Corresponding 5% damped spectra.

code for UCSD. As an example, the resulting acceleration spectra in the EW and NS directions are shown in Fig. 18 for UCR. These results call for the following comments:

- as known from earthquake records where directivity is apparent, some of the synthesized motions show substantial differences between different horizontal directions. This is to be expected at the three campuses, because of their proximity to the causative faults.
- the properties of the sites may emphasize specific spectral periods. This may impact negatively the design of structures with certain height and stiffness properties. Typically, the peaked nature of the actual spectra is not represented by the smooth spectra resulting from Probabilistic Spectral Hazard Analyses (PSHA).
- building code guidance allows for using assumptions representative of the mean when numerous motion time-histories are available for a site. In that case one would be underestimating the severity of the motions in half of the potential earthquakes. The CEP results show that the underestimation could be very significant. Clearly, even for a given magnitude event on a given fault, one will never know the severity of the largest possible rupture scenario. A stochastic deterministic approach, such as used in the CEP studies, can provide a realistic upper bound estimate for a very large percentage of rupture scenarios.

The CEP-estimated ground motions relate to campuses that are only a few kilometers away from fault segments capable of producing M 6.8 to 7.0 earthquakes. In general, these estimates are substantially stronger than those currently adopted for the campuses. In order to 'calibrate' the severity of the estimated accelerations we show a sample comparison, for UCR, of these CEP results with acceleration spectra corresponding to stations at comparable distances from three recent events of somewhat comparable magnitude in California (Fig. 19). These comparisons indicate that the CEP-estimated motions are not overestimates.

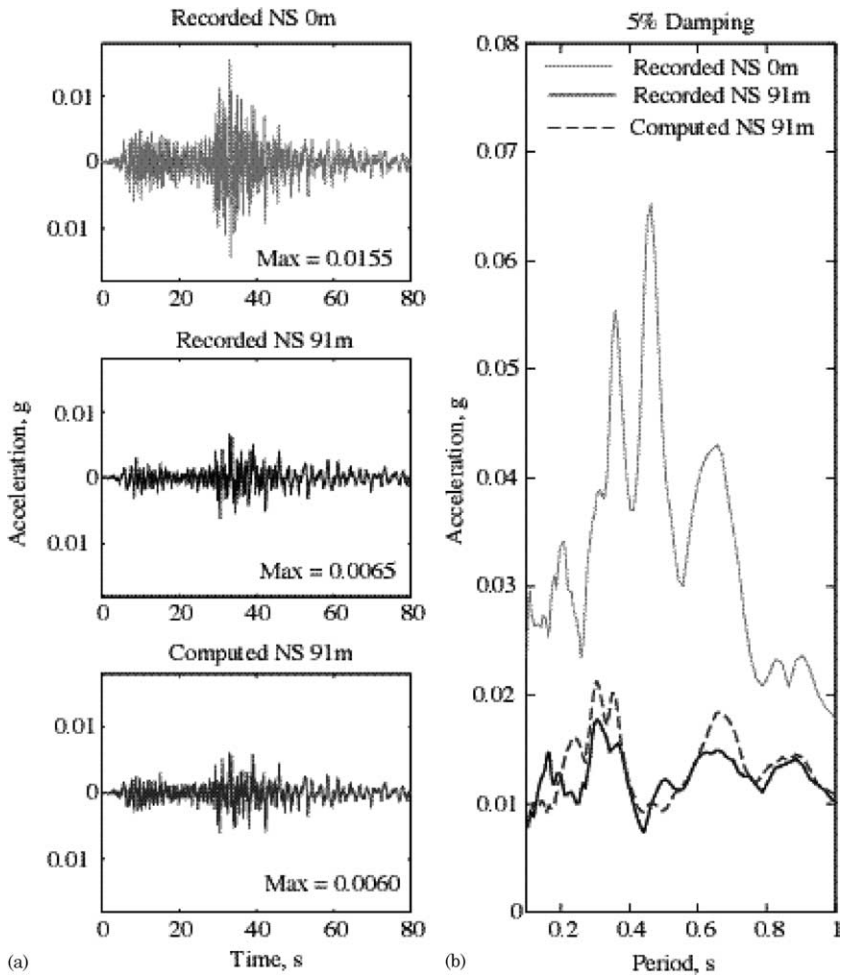

Fig. 15. (a) Calculated vs. recorded horizontal motions, at UCSD at 91-m depth, for the NS component of the October 16, 1999 Hector Mine earthquake (M 7.1 at 134 km); (b) Corresponding 5% damped spectra.

7. Comparisons of the state-of-the-practice, CEP, and design-basis estimates

7.1. State-of-the-practice estimates

Typically, one would obtain ground motion estimates for the campus sites by using other approaches. One is the 1997 Uniform Building Code (UBC 97) procedure. The outcome is shown in Fig. 20 for all campuses, for 5% damping and for a Soil C site condition. These spectra are based on the results of the CEP geophysical logging, and on the relevant causative fault(s) (see International Conference of Building Officials/ICBO [33]). We also show the General Procedure Response Spectrum based on the 2000 International Building Code (ICBO [34]). Another approach is to obtain estimates from Probabilistic Seismic Hazard Analyses (PSHA), such as those based on the research of the California Department of Mines and Geology [35,36]. The results are also shown in Fig. 20 for recurrence probabilities of 10, 5, and 2% in 50 years (return periods of 475, 950, and 2375 years, respectively). It is noteworthy that there are some very substantial differences between the spectra obtained by the Building codes and by PSHA for these three sites. For example, the IBC/UBC spectra are well under the 950-year PSHA spectrum at UCR, comparable to it at UCSB, and well above it at UCSD. These discrepancies highlight the simplified nature and the lack of true site-specificity of some of those state-of-the-practice (SOP) methods. This can be a source of concern for designers when needing to choose a basis for earthquake-resistant design.

7.2. Comparison of the CEP and state-of-the-practice estimates

The CEP surface motions are then compared to those based on SOP methods in Figs. 21–23. The comparisons are for horizontal directions on the three campuses. At UCR, the horizontal motions corresponding to the mean CEP estimates are at least as strong as those corresponding to the PSHA estimates for a 950-year return period event. In the period range of 0.1–0.5 s, they are significantly higher (20–50%) than those corresponding to the UBC 1997 spectra. The 84th percentile CEP estimates are comparable

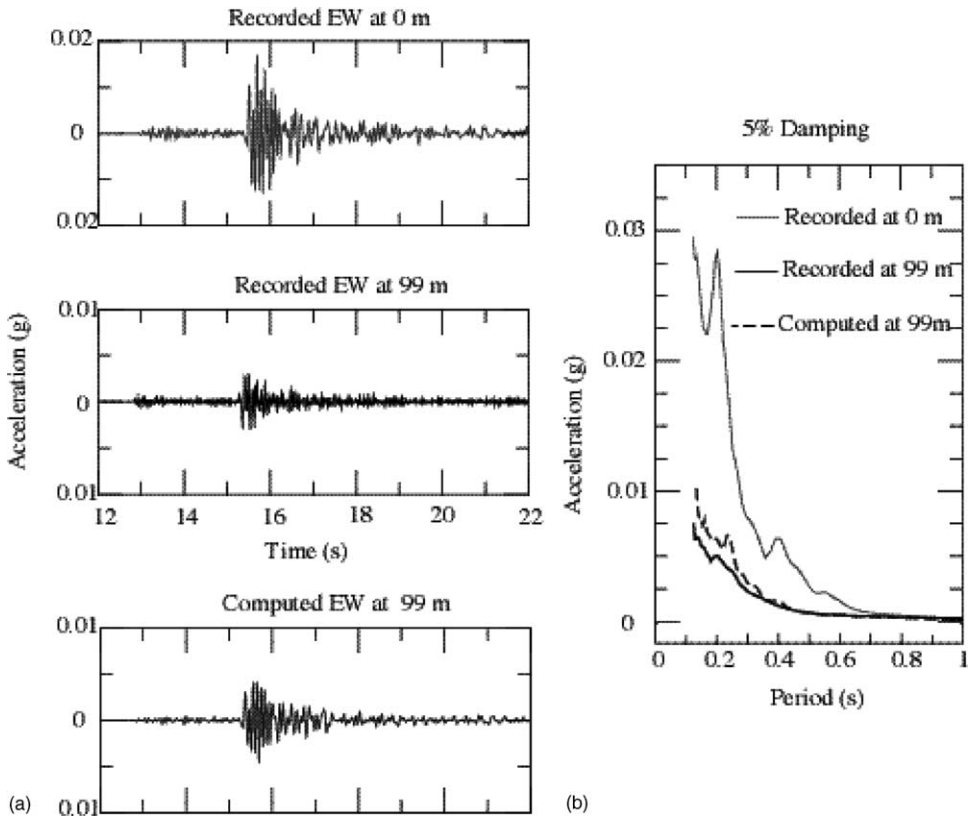

Fig. 16. (a) Calculated vs. recorded horizontal motions, at UCR, at 99-m depth, for the EW component of the March 22, 1999 earthquake (M 3.8 at 8 km); (b) Corresponding 5% damped spectra.

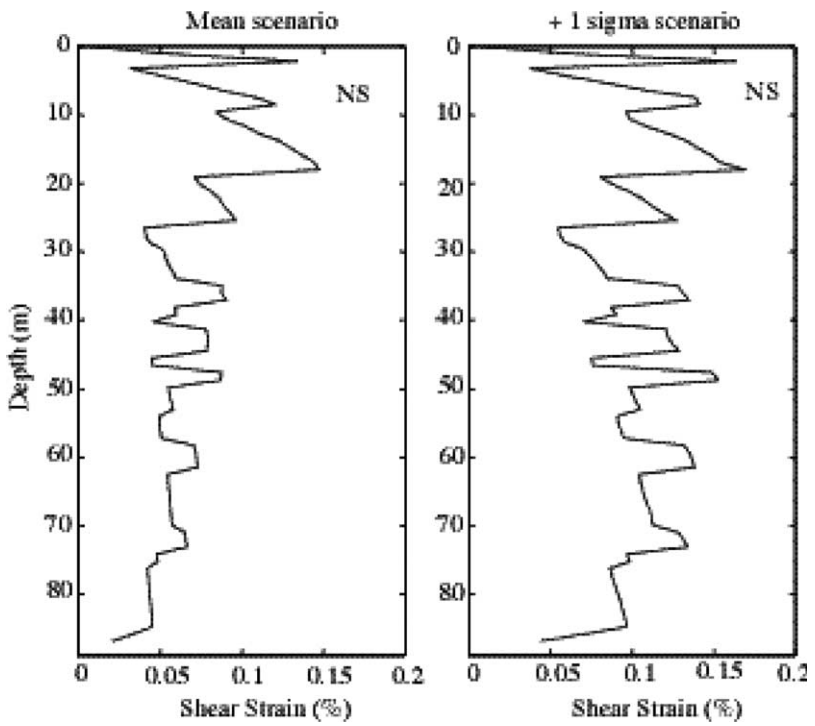

Fig. 17. Maximum shear strains (NS direction) in the soil column at UCR under a M 7.0 event.

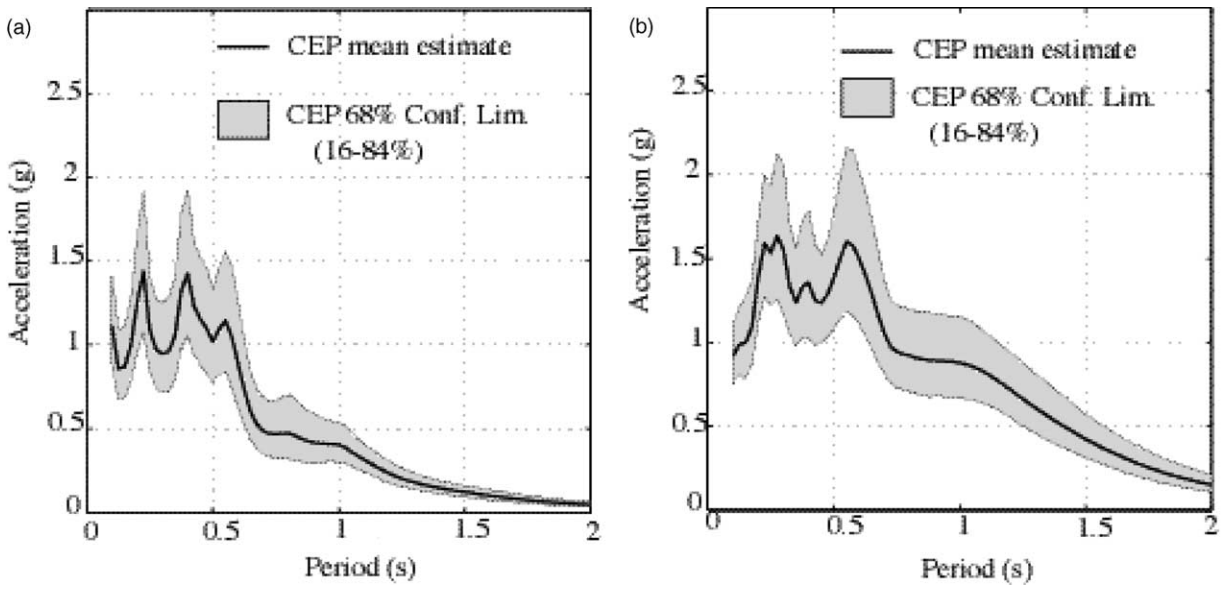

Fig. 18. Horizontal 5% damped acceleration spectra for surface strong motions at UCR, under a M 7.0 event: (a) EW component, (b) NS component.

to the estimates from a 2375-year return period PSHA analysis. At UCSB, the mean of the CEP surface motion estimates is generally comparable to PSHA estimates for a 475-year return period event. In the 0.1–0.5 s period interval, the 84th percentile CEP motions tend to exceed ground motions for a 950-year return period PSHA event. The acceleration spectrum of that 950-year event is generally comparable to the UBC 97 spectrum. Only one in six M 6.8 NCPP earthquakes would be expected to exceed this level of motion. At UCSD, the UBC code-based spectrum accommodates a large portion of the exposure defined by the CEP study. In the range of 0.1–0.5 s,

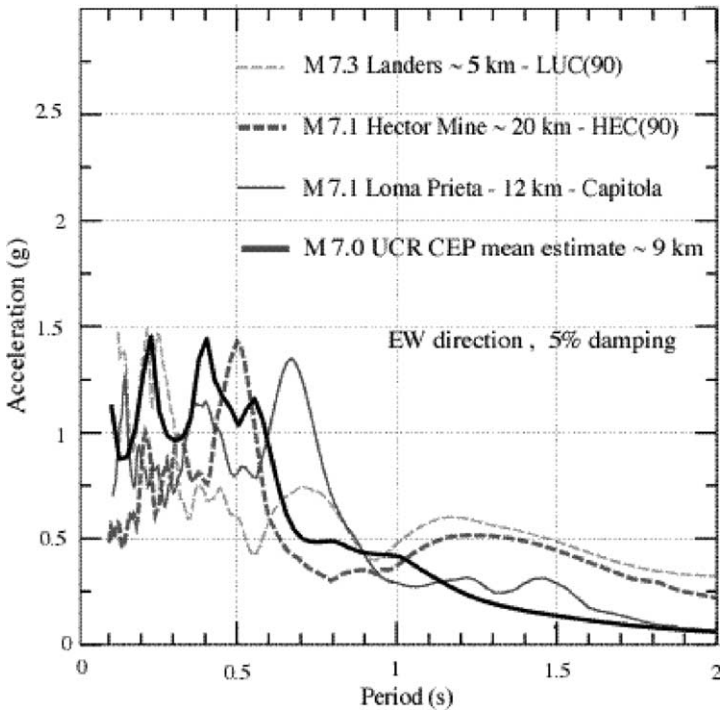

Fig. 19. Horizontal acceleration spectra (EW) for recent M ~ 7 earthquakes in California at ranges comparable to the distance from the campuses to their causative faults, compared to the mean CEP for UCR.

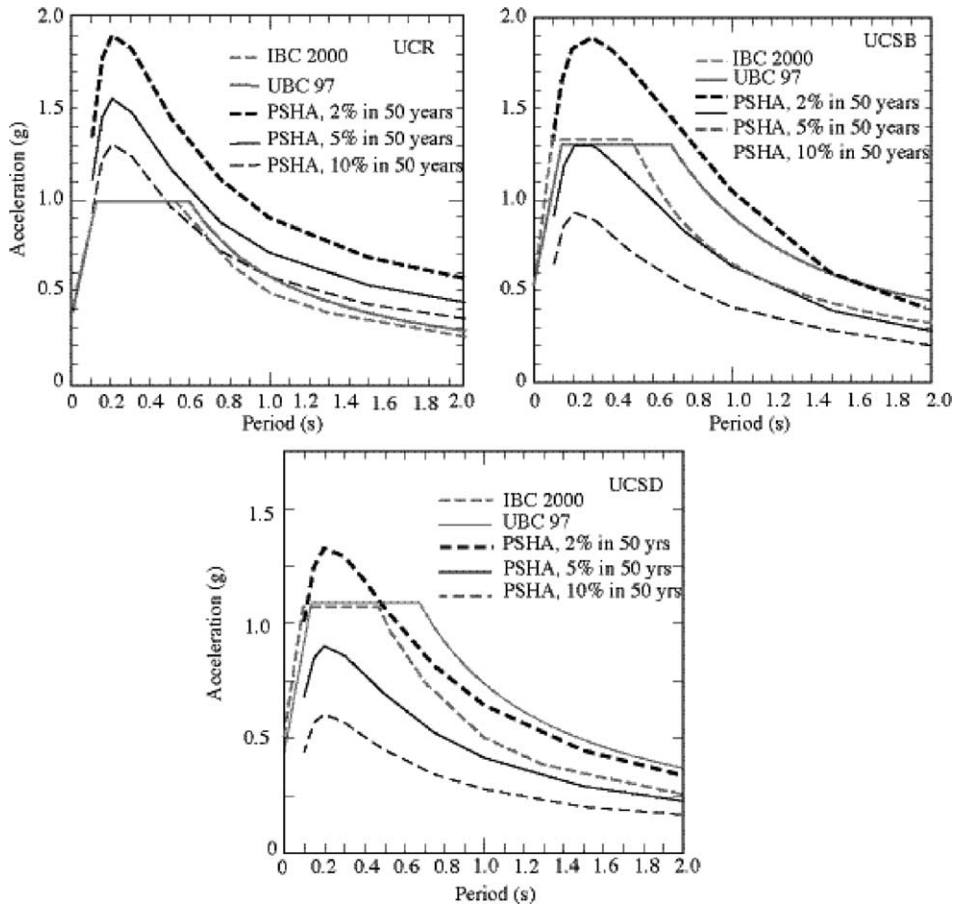

Fig. 20. Horizontal spectral accelerations available from the state-of-the-practice for the three UC campuses studied by the CEP (soil type C; 5% damping).

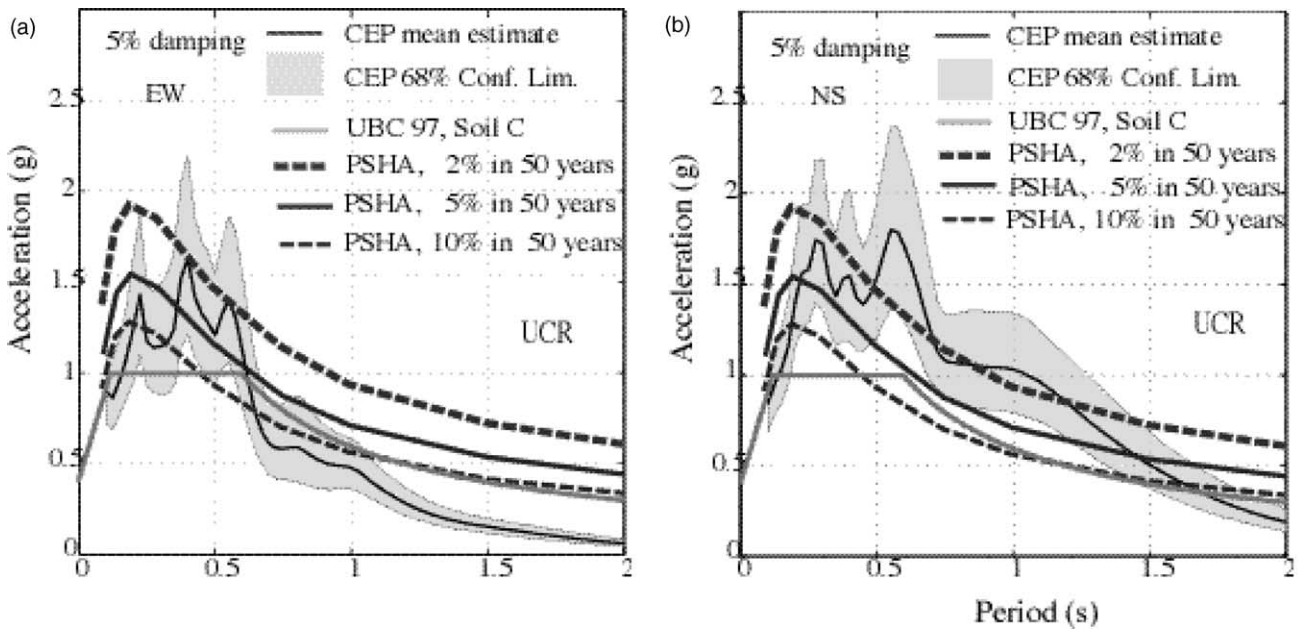

Fig. 21. Comparison of the CEP and state-of-the-practice horizontal spectral accelerations, at UCR: (a) EW component; (b) NS component.

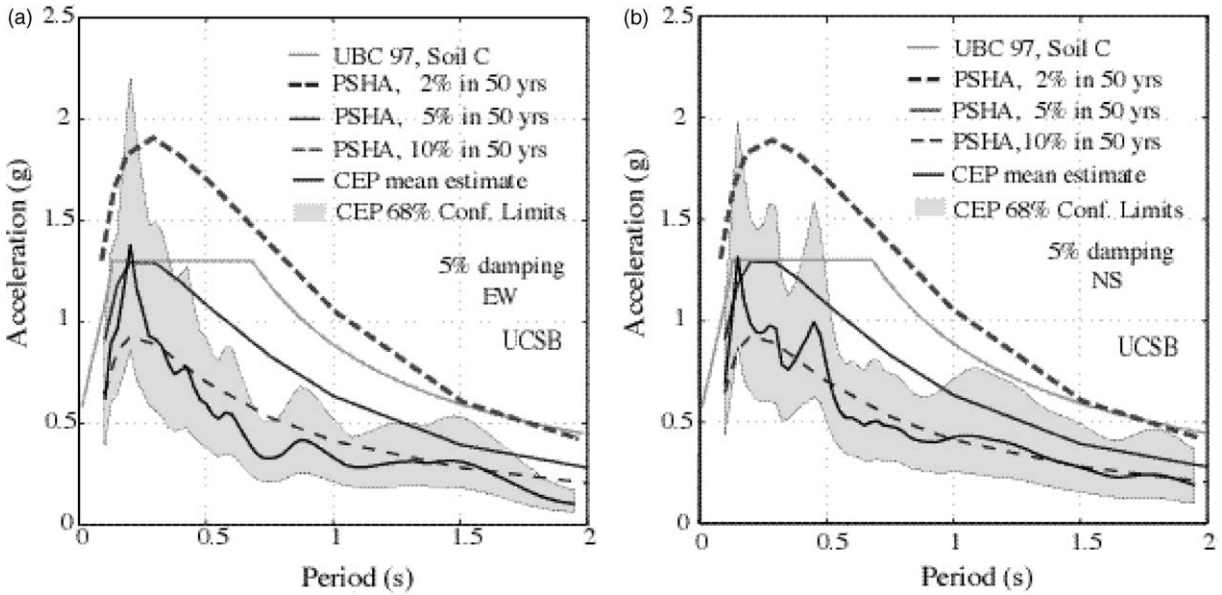

Fig. 22. Comparison of the CEP and state-of-the-practice horizontal acceleration spectra at UCSB: (a) EW component; (b) NS component.

the mean CEP is between the 475 and 950-year event PSHA spectra, and the 84th percentile CEP is generally between the 950 and 2375-year event PSHA spectra.

7.3. Comparison of campus design-basis earthquakes to the CEP estimates

The CEP/design-basis earthquakes (DBE) comparisons are shown in Fig. 24 with reference to the EW direction on each campus. At UCR, the 1997 Design-Basis spectrum used in the retrofit of the Rivera library is considerably lower (a factor of 2) than the CEP mean estimate in the range of 0.1–0.6 s. At UCSB, the 1994 Design-Basis spectrum used for the Engineering I building retrofit was updated in 1999 to be the spectrum of a 475-year PSHA event. This means that 50% of the M 6.8 expected earthquakes on the NCPP fault would create ground motions exceeding the current DBE. At UCSD, the 1989 DBEs used for Thornton hospital, show that the maximum credible event is well in excess of the $+1\sigma$ CEP spectrum and thus covers a very large part of all

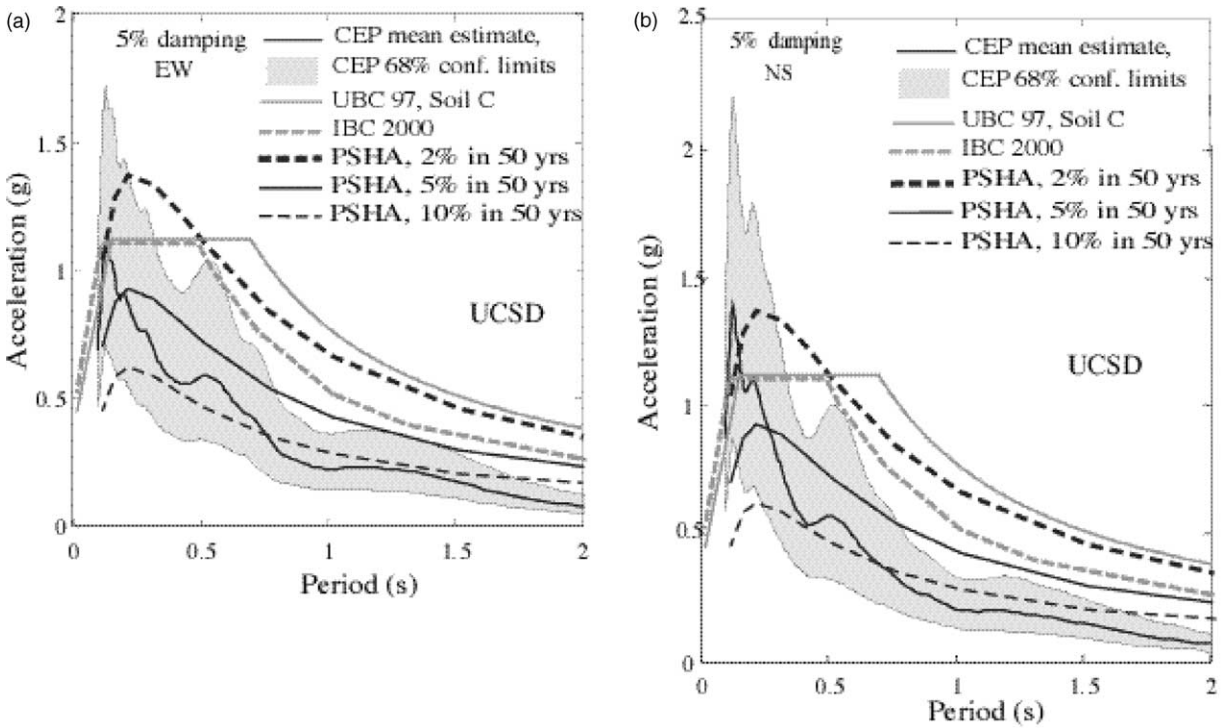

Fig. 23. Comparison of the CEP and state-of-the-practice horizontal acceleration spectra at UCSD: (a) EW component; (b) NS component.

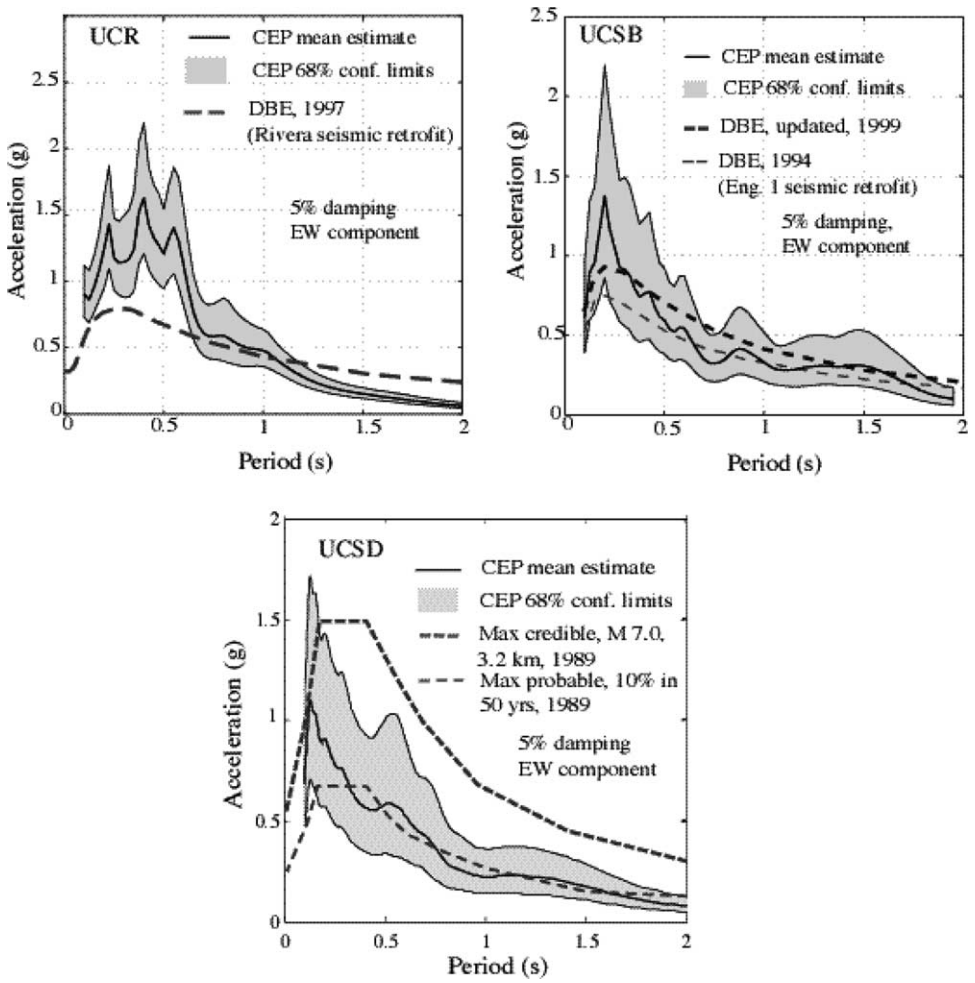

Fig. 24. Comparisons of the CEP estimates and Design-Basis assumptions at the three campuses.

the scenarios considered in the CEP study. The maximum probable event, on the other hand, is substantially underestimating the range of estimated CEP motions.

8. Summary—conclusions

Extensive geological, geophysical, seismological, and geotechnical studies performed on three campuses of the UC have provided new, site-specific estimates of the strong motions that can be expected from earthquakes of moment magnitudes 6.8–7.0 on faults in the vicinity of these campuses. Results for each campus are summarized as follows:

At UCR,

- the motions estimated at the three UCR sites are generally comparable. Because these sites have a fairly deep (more than 60 m) soil cover over the granite bedrock, it is expected that these CEP motions will be representative of those that could be expected at other campus locations where the soil cover is in excess of say 30 m. Motions at locations with shallower bedrock could be expected to be less severe because of a smaller amplification of bedrock motions by the soil profile;
- the horizontal motions corresponding to the mean CEP estimates are at least as strong as those corresponding to the PSHA estimates for a 950-year return period event. In the period range of 0.1–0.5 s they are significantly higher (20–50%) than those corresponding to the UBC 1997 or the IBC 2000 spectra;
- the 1997 Design-Basis spectrum used in the retrofit of the Rivera library is considerably lower (a factor of 2) than the CEP mean estimates in the period range 0.1–0.5 s, and is substantially lower than the UBC, IBC, and 475-year return PSHA event;
- the 84th percentile CEP estimates are comparable to the estimates from a 2375-year return period PSHA analysis;
- the motions estimated by the CEP are very consistent with records from recent earthquakes of comparable magnitudes in California (Hector Mine, Landers, and Loma Prieta);
- these results have instigated a re-examination of earthquake ground motion assumptions at UCR.

At UCSB,

- the 1999 DBE motions for the campus (10% in 50-years probability of occurrence, or 475-year return period) are generally consistent with the mean of the CEP surface motion estimates. This means that 50% of the M 6.8 expected earthquakes on the NCPP fault would create ground motions exceeding the current DBE.
- In the 0.1–0.5 s period range, the 84th percentile of the CEP motions tends to exceed the motions for a 950-year PSHA event. The acceleration spectrum of that 950-year event is very close to the new IBC 2000 spectrum for UCSB, and generally comparable to the UBC 97 spectrum. Only one in six M 6.8 NCPP earthquakes would be expected to exceed this level of motion.
- These results have also prompted a re-examination of earthquake ground motion assumptions at UCSB.

At UCSD,

- The motions estimated at two sites on either side of Interstate 5 (Thornton hospital and PL 601) are generally comparable. These motions are expected to be representative of those that could be expected at other campus sites where the soil profile is comparable.
- However, prior to assuming the same motions for the site of a new construction project or retrofit, it is advisable to determine the shear- and compressional-wave velocities in the top 40 m or so of depth in order to verify the similarity with the sites studied under the CEP. The preferred method for these measurements is the suspension logging described in this paper. This type of investigation would add only a modest cost to standard geotechnical investigations.
- The UBC and IBC code-based spectra accommodate a large portion of the exposure defined by the CEP study. In the range of 0.1–0.5 s, the mean CEP is between the 475 and 950-year event PSHA spectra, and the 84th percentile CEP is generally between the 950 and 2375-year event PSHA spectra.
- The comparison of the CEP estimates to the design basis earthquakes used for Thornton hospital shows that the maximum credible event is well in excess of the $+1\sigma$ CEP spectrum and thus covers a very large part of all the scenarios considered in the CEP study. The maximum probable event, on the other hand, is substantially underestimating the range of estimated CEP motions. In consequence, the seismic design-basis assumptions for UCSD are being re-examined in consultation with the campus geotechnical and structural consultants.
- A comparison of the CEP-estimated acceleration spectra and acceleration time-histories to those from recent strike-slip events in California of comparable magnitude to that assumed for the Rose Canyon fault indicates that the CEP motions are not overestimates.

The extensive studies performed under the CEP clearly indicate that the site-specific CEP estimates should be considered, together with the SOP methods, to arrive at safe and rational decisions concerning the selection of DBEs for buildings on U.C. campuses. The CEP approach is consistent with the current trend towards performance-based design of buildings using time-histories of ground motion. The U.C. system is now building on these results to reassess strong motion exposure at the three campuses.

Acknowledgements

The UC/CLC Campus Earthquake Program was funded from several sources: the U.C. Office of the President, the University Relations Program at LLNL, and the offices of the appropriate Vice-Chancellors on the various campuses. The authors are very grateful for that support.

We also acknowledge the contributions from our colleagues J. Ake (USBR), C. Alex (UCSB), A. Balakrishnan (UCD), E. Cochran (UCSB), S. Elrick (UCR), G. Ely (UCSB), R. Funk (UCR), L. Gurrola (UCSB), B. Kutter (UCD), D. McCallen (LLNL), C. Nicholson (UCSB), C. Pearson (LANL), M. Petersen (USGS), S. Swain (UCSB), and T. Tyler (UCSB).

References

[1] Archuleta R, Nicholson C, Steidl J, Gurrola L, Alex C, Cochran E, Ely G, Tyler T. Initial source and site characterization studies for the U.C. Santa Barbara Campus. Lawrence Livermore National Laboratory report UCRL-ID-129196; December 1997 (http://www.llnl.gov/tid/lof/documents/pdf/232770.pdf).

[2] Park S, Elrick S, Funk R. Initial source and site characterization studies for the U.C. Riverside Campus. Livermore National Laboratory report UCRL-ID-134610; July 1999 (http://www.llnl.gov/tid/lof/documents/pdf/236189.pdf).

[3] Minster B, Wagoner J, Mellors R, Day S, Park S, Elrick S, Vernon F, Heuze F. Initial source and site characterization studies for the U.C. San Diego Campus. Lawrence Livermore National Laboratory report, UCRL-ID-134785; July 1999 (http://www.llnl.gov/tid/lof/documents/pdf/236207.pdf).

[4] Archuleta R, Bonilla F, Doroudian M, Elgamal A, Heuze F, Hoehler M, Lai T, Lavallee D, Liu P-C, Martin A, Riemer M, Steidl J, Vucetic M, Yang Z. Strong earthquake motion estimates for the UCSB Campus, and related response of the Engineering I Building. Lawrence Livermore National Laboratory report, UCRL-ID-138641; August 2000. 84 p. (http://www.llnl.gov/tid/lof/documents/pdf/238259.pdf).

[5] Archuleta R, Elgamal A, Heuze F, Lai T, Lavallee D, Lawrence B, Liu P-C, Matesic L, Park, S, Riemer M, Steidl J, Vucetic M, Wagoner J, Yang Z. Strong earthquake motion estimates for three sites on the U.C. Riverside Campus. LLNL report, UCRL-ID-140522; November 2000. 68 p. (http://www.llnl.gov/tid/lof/documents/pdf/238854.pdf).

[6] Day S, Doroudian M, Elgamal A, Gonzales S, Heuze F, Lai T, Minster B, Ogelsby D, Riemer M, Vernon F, Vucetic M, Wagoner J, Yang

Z. Strong earthquake motion estimates for three sites on the U.C. San Diego Campus. LLNL report, UCRL-ID-140523; May 2002. 51 p. (http://www.llnl.gov/tid/lof/documents/pdf/240884.pdf).
[7] Working Group on California Earthquake Probabilities, Seismic hazards in Southern California: probable earthquakes, 1994 to 2004. Bull Seismol Soc Am 1995;85(2):379–439.
[8] Doroudian M, Vucetic M. A direct simple shear device for measuring small strain behavior. ASTM Geotech Test J 1995;18(1):69–85.
[9] Dobry R, Vucetic M. Dynamic properties and seismic response of soft clay deposits. Proceedings International Symposium on Geotechnical Engineering of Soft Soils, Mexico City, vol. 2. Mexico City, Mexico: Sociedad Mexicana de Mecanica de Suelos; 1987. p. 49–85.
[10] Vucetic M, Dobry R. Effect of soil plasticity on cyclic response. ASCE J Geotech Engng 1991;117(1):89–107.
[11] Matesic L, Vucetic M. Strain-rate effects on soil's secant shear modulus at small cyclic strains. ASCE J Geotech Geoenviron Engng 2003;129(6).
[12] Pitilakis KD, Anastasiadis AJ. Soil and site characterization for seismic response analysis. Proceedings of the 11th European Conference on Earthquake Engineering, Paris, France, September 6–11, Brookfield, VT: A.A. Balkema; 1998. p. 65–90.
[13] Hardin BO, Black WL. Vibration modulus of normally consolidated clay. ASCE J Soil Mech Found 1968;94(SM2):353–69.
[14] Riemer MF, Abu-Safaqah O. Large-strain triaxial testing of soil samples from U.C. San Diego. U.C. Berkeley Geotechnical Engineering Division report; July 1999. 17 p.
[15] Heuze FC, Ueng T-S, Hutchings LJ, Jarpe SP, Kasameyer PW. A coupled seismic-geotechnical approach to site-specific strong motion. Soil Dyn Earthq Engng 1997;16:259–72.
[16] Aki K, Richards PG. Quantitative seismology, theory and methods, 2 volumes. San Francisco, CA: W.H. Freeman; 1980.
[17] Archuleta RJ, Liu P-C, Steidl JH, Bonilla LF, Lavallee D, Heuze FE. Finite-fault site-specific acceleration time-histories that include nonlinear soil response. Phys Earth Planet Interiors 2003;4190:1–29.
[18] Hartzell SH. Earthquake aftershocks as Green's functions. Geophys Res Lett 1978;5:1–4.
[19] Tumarkin AG, Archuleta RJ. Empirical ground motion prediction. Annali Geofisica 1994;37(6):1691–720.
[20] Pavic R, Kollar MG, Bard P-Y, Lacave-Lachet C. Ground motion prediction with the empirical Green's function technique: an assessment of uncertainties and confidence level. J Seismol 2000;4: 59–77.
[21] Aki K. Scaling law of seismic spectrum. J Geophys Res 1967;72: 1217–31.
[22] Brune JN. Tectonic stress and the spectra of seismic shear waves from earthquakes. J Geophys Res 1970;75:4997–5009. Correction, J Geophys Res 1971;76:5002.
[23] Wald DJ, Heaton TH, Hudnut KW. The slip history of the 1994 Northridge, California earthquake, determined from strong-motion, teleseismic, GPS, and leveling data. Bull Seismol Soc Am 1996;86: S49–S70.
[24] Bonilla LF, Lavallee D, Archuleta RJ. In: Irikura K, et al., editors. Nonlinear site response: laboratory modeling as a constraint for modeling accelerograms. Proceedings Second International Symposium on the Effects of Surface Geology on Seismic Motion, vol. 2. Brookfield, VT: A.A. Balkema; 1998. p. 793–800.
[25] Hartzell S, Harmsen S, Frankel A, Larsen S. Calculation of broadband time-histories of ground motion: comparison of methods, and validation using strong ground motion from the 1994 Northridge Earthquake. Bull Seismol Soc Am 1999;89:1484–504.
[26] Abrahamson N, Becker A, editors. Proceedings of the MCEER Workshop on Ground Motion Methodologies for the Eastern United States. Technical Report MCEER-99-0016, Buffalo, NY: State University of New York; 1999.
[27] Dan K, Watanabe T, Tanaka T, Sato R. Stability of earthquake ground motions synthesized by using different small-event records as empirical Green's functions. Bull Seismol Soc Am 1990;80:1433–55.
[28] Jarpe SP, Kasameyer PK. Validation of a procedure for calculating broadband strong-motion time-histories with empirical Green's functions. Bull Seismol Soc Am 1996;86:1116–29.
[29] Somerville PG, Smith NF, Graves RW, Abrahamson NA. Modification of empirical strong ground motion attenuation relations to include the amplitude and duration effects of rupture directivity. Seismol Res Lett 1997;68:199–222.
[30] Oglesby DD, Day SM. Stochastic fault stress: implications for fault dynamics and ground motion. Bull Seism Soc Am 2002;92:3006–21.
[31] Li XS, Wang ZL, Chen CK. SUMDES: a nonlinear procedure for response analysis of horizontally-layered sites subjected to multi-directional earthquake loading. Davis: Department of Civil Engineering, University of California; 1992. p. 86.
[32] Elgamal A, Yang Z, Parra E. Computational modeling of cyclic mobility and post-liquefaction site response. Soil Dyn Earthq Engng 2002;22(4):259–71.
[33] International Conference of Building Officials/ICBO Maps of Known Active Fault Near-Source Zones in California and Adjacent Portions of Nevada. ISBN 1-58001-008-3 (ICBO, 5360 Workman Mill Road, Whittier, CA, 90601-2298); 1998.
[34] International Conference of Building Officials/ICBO International Building Code 2000. ISBN 1-892395-25-8, 756 pp., (ICBO, 5360 Workman Mill Road, Whittier, CA, 90601-2298); March 2000.
[35] Petersen M, et al. Probabilistic seismic hazard assessment for the State of California. California Department of Conservation, Division of Mines and Geology, Open-File Report 96-08. Also available as U.S. Geological Survey Open-File Report 96-706; 1996.
[36] Blake T. FRISKP 3.01b Brochure, 4568 Via Grande, Thousand Oaks, CA 91320-6712; 1999.